Radioactive Decay of Se^{83}†‡

K. W. MARLOW
United States Naval Research Laboratory, Washington, D. C., and University of Maryland, College Park, Maryland
AND
M. A. WAGGONER
University of Maryland, College Park, Maryland and University of Iowa, Iowa City, Iowa
(Received 9 January 1967; revised manuscript received 21 June 1967)

The radioactive decay of Se^{83} produced by $Se^{82}(n,\gamma)$ has been investigated experimentally, leading to a proposed level scheme for Br^{83}. The half-life of the long-lived decay was determined to be 22.6±0.2 min, and the 70-sec half-life of Se^{83m} was confirmed. For the long-lived decay, the various coincidence studies lead to a proposed decay scheme incorporating 29 γ rays and involving excited levels in Br^{83} at 356, 801, 868, 1094, 1355, 1421, 1438, 1814, 2060, 2650, 2697, 2738, and 2777 keV. The 1094-keV level has been found to have $T_{1/2}=4.1\pm0.1$ nsec. Although coincidence measurements have not been made in the study of the short-lived isomer, β- and γ-ray spectrum measurements lead to the placement of nine γ rays in the proposed decay scheme, with excited levels at 356, 1032, 1063, 2022, 2054, and 2147 keV. Logft values, determined from the studies of β-ray spectra, have been used to limit spin and parity assignments for many of the levels, while lifetime and directional correlation measurements have provided further limitations on the assignments for a few levels.

I. INTRODUCTION

WE have observed that the odd-mass nuclei with atomic number (Z) between 28 and 50 have generally been inadequately described theoretically and experimentally. Within the past few years the core-excitation model[1–11] has undergone a considerable amount of development in order to provide an accurate description of the excited levels of odd-mass nuclei. But the core-excitation model has been applied almost exclusively to the odd-mass isotopes of copper ($Z=28$). We have undertaken a detailed study of the excited levels of Br^{83} ($Z=35$), not only to provide a good experimental description of a nucleus whose proton number lies between the shell closures at 28 and 50 protons, but also to provide the basis for a test of the predictions of the core-excitation model with the observed properties of such a nucleus. Our preliminary investigations and the earlier work of others[12–15] had indicated that the decay of Se^{83} (which populates the levels of Br^{83}) was not accurately described. Since the ground level of Br^{83} is unstable, the excited levels cannot be studied by the Coulomb-excitation technique; further, the levels cannot be studied by the (d,p) or (n,γ) reactions since Br^{82} is an unstable nucleus. We have utilized the β decay of the isomeric levels of Se^{83} as a means of populating the levels of Br^{83}.

II. REVIEW OF PREVIOUS WORK

The net result of the work on Se^{83} prior to 1958 was essentially that two isomeric activities were known to exist with half-lives of approximately 70 sec and 25 min.[16–20] In 1958 Cochran and Pratt[12] reported on a study of the short-lived isomer of Se^{83}. Samples of selenium enriched to 75.7% in Se^{82} were irradiated in the neutron flux of a nuclear reactor and yielded Se^{83} by the (n,γ) reaction. γ rays with energy 350, 650, 1010 (double), and 2020 keV from an activity decaying with $T_{1/2}=70\pm1$ sec were observed, and they recorded γ-ray spectra in coincidence with γ rays of selected energy and β-ray spectra in coincidence with γ rays of selected energy. On the basis of these measurements they stated that the β-ray transition energy was approximately 1500 keV and proposed a decay scheme. Cochran and Pratt[13] later investigated the long-lived isomer of Se^{83} for which they obtained $T_{1/2}\approx25$ min. Gamma rays were observed with energies of 225, 358, 524, 712, 833, 1058, 1309, 1880, and 2294 keV. β-ray spectrum measurements were less precise than those for γ rays but transitions were reported with energies

† This work was supported by the Naval Research Laboratory, Washington, D. C.
‡ This article contains material abstracted from a dissertation presented by K. W. Marlow to the Graduate School of the University of Maryland in partial fulfillment of the requirements of the degree Doctor of Philosophy, 1966.

[1] R. D. Lawson and J. L. Uretsky, Phys. Rev. **108**, 1300 (1957).
[2] A. de-Shalit, Phys. Rev. **122**, 1530 (1961).
[3] A. Braunstein and A. de-Shalit, Phys. Letters **1**, 264 (1962).
[4] J. Vervier, Nuovo Cimento **28**, 1412 (1963).
[5] B. F. Bayman and L. Silverberg, Nucl. Phys. **16**, 625 (1960).
[6] M. Harvey, Nucl. Phys. **48**, 578 (1963).
[7] M. Bouten and P. van Leuven, Nucl. Phys. **32**, 499 (1962).
[8] V. K. Thankappan and W. W. True, Phys. Rev. **137**, 793 (1965).
[9] W. Beres (unpublished).
[10] W. Beres, Phys. Letters **16**, 65 (1965).
[11] W. Beres, Nucl. Phys. **68**, 49 (1965).
[12] R. G. Cochran and W. W. Pratt, Phys. Rev. **109**, 878 (1958).
[13] R. G. Cochran and W. W. Pratt, Phys. Rev. **113**, 852 (1958).
[14] C. Ythier and R. van Lieshout, J. Phys. Radium **21**, 470 (1960).
[15] K. W. Baskova, S. S. Vasil'ev, No Seng-Ch'ang, and L. Ya. Shavtvalov, Zh. Eskperim. i Teor. Fiz. **42**, 416 (1962) [English transl.: Soviet Phys.—JETP **15**, 289 (1962).
[16] A. H. Snell, Phys. Rev. **52**, 1007 (1937).
[17] A. Langsdorf and E. Segrè, Phys. Rev. **57**, 105 (1940).
[18] L. E. Glendenin, Nat. Nucl. Energy Ser., Div. **11**, **9**, 592 (1950), editor's note.
[19] J. R. Arnold and N. Sugarman, J. Chem. Phys. **15**, 703 (1947).
[20] W. C. Rutledge, J. M. Cork, and S. B. Burson, Phys. Rev. **86**, 775 (1952).

450, 1000, and 1700 keV. Some γ-γ coincidence spectra were recorded and the following coincidences reported: 358–2294, 358–1309, and 524–1880. In an attempt to improve on their previous work on the 70-sec isomer, they measured the β-ray spectra and reported β-ray transitions of 1750 and 3750 keV. Ythier and van Lieshout[14] produced the Se^{83} activity by means of the (d,p) reaction with 10-MeV deuterons on a target of selenium enriched to 87% in the mass-82 isotope. Chemical separations were performed to remove other reaction products. The chief distinctions between their results and those of Cochran and Pratt[13] are the following: The 524-keV γ ray decays with $T_{1/2}=2.3$ h and therefore belongs to the decay of Br^{83}; the 2294–225–358-keV γ-ray cascade is not correct, the 830-keV γ ray is double (805 and 900 keV), and other γ rays exist (1228 keV, etc.). Measurements made in a total-absorption scintillation spectrometer indicated energy levels at 2710, 3030, and 3265 keV.

Baskova *et al.*[15] reported somewhat different results on the decay of Se^{83}. They also produced their sources by the (d,p) reaction with 9-MeV dueterons incident upon selenium enriched to 74.6% in the mass-82 isotope. No chemical separation was performed, however. They observed the decay, with $T_{1/2}=25\pm1$ min, of an activity with four γ-ray transitions having energies 220, 355, 1850, and 2300 keV, and with three β-ray transitions having energies (and relative abundance) 1000 keV (58%), 1800 keV (40%), and 3300 keV (2%). They found no γ ray in coincidence with the 3300-keV β ray. They attributed all of the other γ rays observed (530, 780, 1060, 1300, and 1480 keV) to Br^{83}. Baskova *et al.* were unable to construct a decay scheme based on their evidence.

III. SOURCE PREPARATION

The radioactive Se^{83} for the present study was produced by the reaction $Se^{82}(n,\gamma)Se^{83}$ using elemental selenium enriched in Se^{82}. Samples with two different enrichments were used. One had Se^{82} (89.9%), Se^{80} (6.2%), Se^{78} (2.2%), Se^{77} (0.7%), Se^{76} (0.9%), and Se^{74} (0.1%). The other had Se^{82} (75.7%), Se^{80} (13.9%), Se^{78} (5.9%), Se^{77} (1.9%), Se^{76} (2.3%), and ^{74}Se (0.3%). Although most of the measurements were made with the samples enriched to 90% in Se^{82}, no significant difference was observed in the results of measurements made on samples of the two different enrichments.

For γ-ray measurements approximately 2 mg of the elemental, enriched selenium was heat-sealed in a small hole drilled in one end of a polyethylene rod 3 mm in diameter by 12-mm long. For measurement of β radiation, approximately 2 mg of the finely divided, elemental, enriched selenium was sandwiched between two sheets of polyethylene film 6-μ thick.

The neutrons for the (n,γ) reaction were supplied by the slow neutron fission of uranium in a nuclear reactor at the U. S. Naval Research Laboratory.

IV. γ-RAY SPECTRUM MEASUREMENTS

A. Experimental Arrangement

Gamma-ray spectra were recorded with a commercially available lithium-drifted germanium semiconductor detector[21] which gave enough improvement in the energy resolution over that obtainable with a scintillation spectrometer, that the separation of previously unresolved peaks in the γ-ray spectrum was possible. The depletion layer of the detector used was 5-mm thick and the area 4 cm^2. A 9-mm Lucite β-ray shield was placed in front of the detector for all measurements. The signals from the detector were amplified in a low-noise charge-sensitive preamplifier and amplifier and analyzed by a 512-channel pulse-height analyzer. The detector associated electronic amplification resulted in an energy resolution of approximately 10 keV over the energy region 100 to 2500 keV.

A pulse-height-versus-energy relation was determined with the aid of the well-known energy calibration points of the radioactive sources Ce^{141}, Hg^{203}, Na^{22}, Y^{88}, Cs^{137}, Au^{198}, and Na^{24}. The maximum deviation of the data points from the resultant energy calibration equation was 3.0 keV and the average deviation was 1.4 keV.

In order to determine relative intensities of γ rays, an experimental relative efficiency curve was obtained showing the number of counts in the full-energy absorption peak as a function of energy from approximately 100 to 2800 keV. The ratios of the areas of double-escape and full-absorption peaks was determined for γ rays at 1836, 2615, and 2754 keV, making it possible to determine the contribution of the double-escape process to peaks lying 1022 keV lower than a known full-absorption peak.

Probable errors in relative intensities due to efficiency corrections were of the order of 10% for energies from 150 to 1300 keV, and increased to approximately 25% at 2700 keV.

B. γ-Ray Spectra of the Long-Lived Isomer of Se^{83}

Figure 1 shows a typical γ-ray spectrum obtained with the system described above. Background, including that due to Se^{75} present in the sources, has been subtracted. In the 850- and 1320-keV regions of the spectrum, several peaks (unresolved by earlier workers) now appear to be resolved. In addition, the two prominent γ rays near 2300 keV were previously thought to be only one. Certain of the γ rays in Fig. 1 have been shown to belong to activities different from that of Se^{83}. The peak at 530 keV results from the decay of Br^{83}, the peaks corresponding to 1147, 1645, and 2168 keV are due to Cl^{38} contamination, and the peaks at 104, 274, and 289 keV arise from the decay of Se^{81}.

The relative intensities of the Se^{83} γ rays in Fig. 1 have

[21] G. T. Ewan and A. J. Tavendale, Can. J. Phys. 42, 2286 (1964).

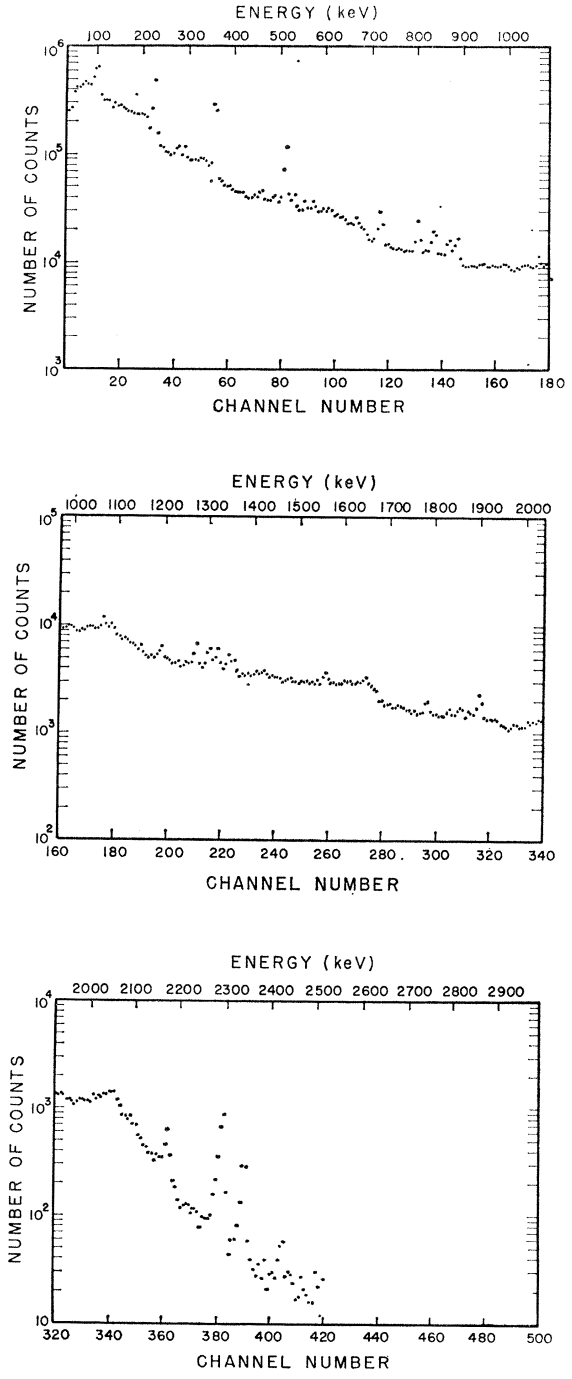

FIG. 1. Gamma-ray spectrum of the long-lived isomer of Se^{83}, recorded by the lithium-drifted germanium detector.

been determined with the aid of the relative efficiency calibration. Separate determinations were made for three different spectra and the average values of the results are shown in Table I. The intensity data have been normalized to 100 for the 356-keV γ rays and allowance has been made for double escape. For comparison, the data of Cochran and Pratt[13] are included in the Table. All energy values quoted in Table I have standard errors of 2 keV.

TABLE I. Energy and relative intensity of γ rays accompanying the decay of the long-lived isomer of Se^{83}.

Energy (keV)	Relative intensity This work	Cochran and Pratt[a]
226	47 ±5	64±9
356	100 ±10	100±23
457	4.8±1.0	
487	3.6±1.0	
512	61 ±6	86±14
554	4.2±1.0	
572	5.9±1.0	
666	3.6±1.0	
720	30 ±3	36±14
801	20 ±2	
837	19 ±2	
868	12.0±1.5	59±9
886	12.0±1.5	
1065	8 ±3	
1082	3 ±1	23±9
1192	6 ±1	
1299	12.0±1.5	
1319	6 ±3	
1344	8 ±1	36±9
1355	4 ±1	
1421	1.0±0.5	
1558	4 ±1	
1784	5 ±1	
1830	1.8±0.5	
1855	4 ±1	
1879	2 ±1	23±9
1897	12.0±1.2	
2088	1.0±0.5	
2291	17 ±3	
2338	5 ±1	14±9
2421	1.0±0.5	

[a] Reference 13.

C. γ-Ray Spectra of the Short-Lived Isomer of Se^{83}

Figure 2 shows a γ-ray spectrum recorded in a study of the 70-sec isomer of Se^{83}. The sources were exposed to neutrons for 1 min, allowed to decay for 2 min, counted on the pulse-height analyzer in the "add" mode for 2 min, allowed to decay one additional minute, and then counted again in the "subtract" mode for 2 min. This procedure subtracted out the effect of constant background and long-lived activities. In a separate measurement, a sequence of γ-ray spectra were recorded to determine whether all peaks decayed with the same half-life. The 94-keV peak decayed with a 3.5-min half-life corresponding to Se^{79} and the 161-keV peak decayed with a half-life considerably shorter than 1 min, and was ascribed to 17.5-sec Se^{77}. The remaining prominent γ rays and their relative intensities are shown in Table II. All γ-ray energy values have standard errors of 2 keV. The intensity of the 1032-keV γ ray has been corrected by approximately 15% for the double-escape peak due to the 2054-keV γ ray. Other weak transitions which may or may not accompany the 70-sec activity have been included in the Table. Several

TABLE II. Energy and relative intensity of γ rays in the decay of the short-lived isomer of Se^{83}.

Energy (keV)	Relative intensity This work	Cochran and Pratt[a]
226	3 ±1	
296	0.5±0.3	
324	1.9±0.5	
356	100 ±10	100
384	1.1±0.5	
444	2.4±1.5	
454	1.0±0.7	
513	3 ±1	
676	86 ±9	160
702	2.4±1.2	
801	3.1±1.5	
883	2.9±1.5	
912	1.0±0.5	
989	96 ±10	
1031	148 ±25	800
1063	[28] ±3	
1116	4.6±2	
1563	6 ±4	
1664	14 ±5	
2054	66 ±10	310
2147	1.1±0.5	
2296	0.7±0.5	

[a] Reference 12.

of the less intense peaks belong to the 23-min decay of Se^{83}.

The simple decay scheme of Cochran and Pratt[12] cannot be supported by the results of this work, summarized in Table II. The relative-intensity data of Cochran and Pratt have been included for comparison. In particular, there are three γ rays near 1000 keV instead of two, and the 2054-keV γ ray cannot be a crossover transition for a cascade which includes the 356- and 676-keV γ rays. A modified decay scheme will be proposed in Sec. XI.

D. Proportional Counter

A proportional counter which permitted the measurement of γ and x rays as low as approximately 3 keV was used in a search for low-energy γ-ray transitions. No high-intensity γ rays in the energy range 3 to 50 keV associated with the decay of the long-lived isomer of Se^{83} were observed.

V. β-RAY SPECTRUM MEASUREMENTS

A. Experimental Apparatus and Methods of Data Correction

For the detection of β rays, commercially available lithium-drifted silicon detectors were used. One of the silicon detectors was 3-mm thick by 10 mm in diameter with the electrons incident upon the flat face. The other detector was 12-mm square and 5-mm thick with the electrons incident upon one of the 5-mm by 12-mm sides.

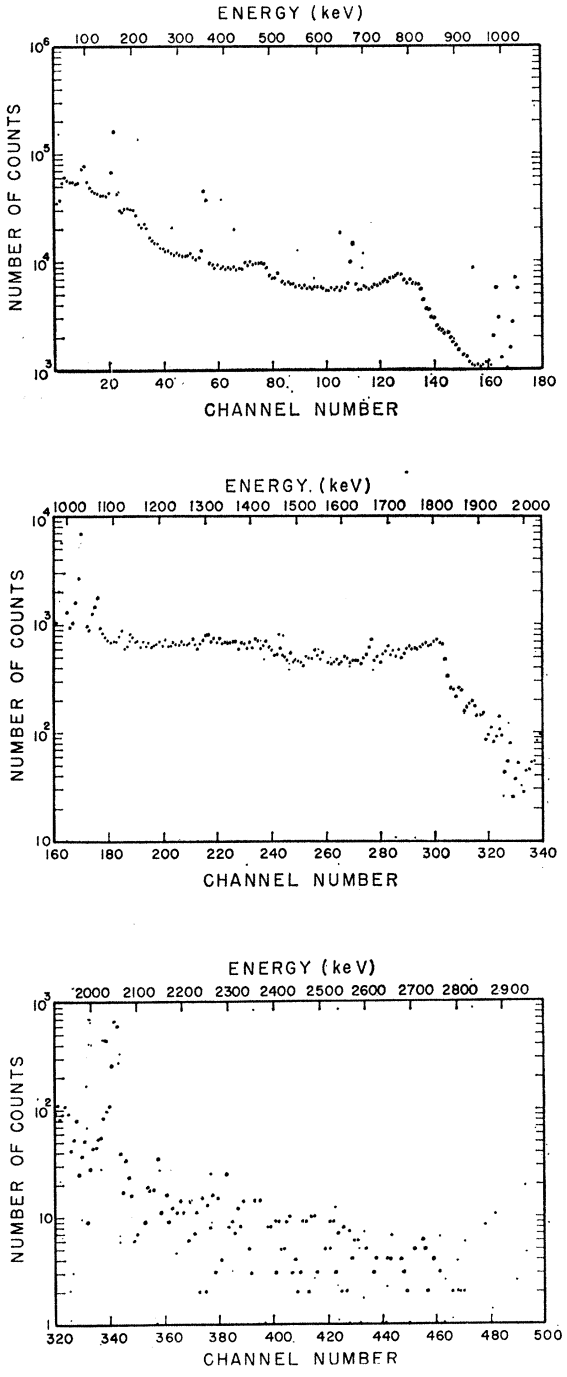

FIG. 2. γ-ray spectrum of the short-lived isomer of Se^{83}, recorded by the lithium-drifted germanium detector.

A meaningful analysis of the β-ray spectra obtained with these detectors required the correction of the measured spectra for the back-scattering effect.[22,23] Similar problems have been previously treated for β-ray

[22] B. P. Burtt, Nucleonics 5, 28 (1949).
[23] R. D. Birkhoff, *Handbuch der Physik*, edited by S. Flügge (Julius Springer-Verlag, Berlin, 1958), Vol. 34, p. 132.

scintillation spectrometer data[24,25] and methods used there have been used as a guide here.

Conversion-electron line shapes were helpful in obtaining a simple mathematical representation of the pulse-height spectrum of a monoenergetic source of electrons (see, for an example, Fig. 3). It was found convenient to treat all of the peak counts as though they occurred in a single channel of the pulse-height spectrum and to represent the tail as a constant-height distribution. Since a linear relationship exists between the energy E and the pulse-height analyzer channel number h, we used h as a unit of energy. If h' corresponds to the energy of incident monoenergetic electrons, we represent the normalized spectrum recorded by the detector as

$$L(h,h') = \frac{1}{(\alpha-1)+(\beta+1)h'}, \quad \text{for} \quad h<h'$$

$$= \frac{\alpha+\beta h}{(\alpha-1)+(\beta+1)h'}, \quad \text{for} \quad h=h'$$

$$= 0, \quad \text{for} \quad h>h'$$

where $(\alpha+\beta h')$ is the ratio of the number of counts in the peak to the number of counts in each of the lower-energy channels. For a given experimental apparatus, the two constants α and β must be fixed. The determination of the constants α and β was by trial-and-error method. The criterion for selection of the appropriate constants was that the corrected spectra of β-ray transitions known to have an allowed shape, but with widely differing end points, would result in allowed Fermi plots which were straight over a large part of the energy range. Figure 4 demonstrates the application of such an analysis to the β spectra of Au^{198}, Na^{24}, and In^{114m}.

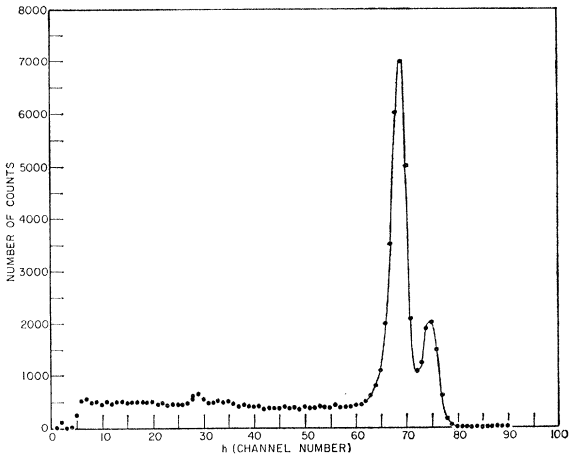

FIG. 3. Electron spectrum of the 1063-keV transition in Pb^{207} in coincidence with the 570-keV γ ray, recorded with the small lithium-drifted silicon detector.

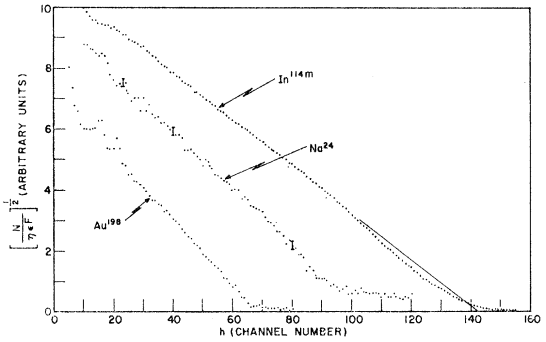

FIG. 4. Fermi plots of the allowed β-ray spectra of Au^{198}, Na^{24}, and In^{114m}; from data recorded with the small lithium-drifted silicon detector.

Since the range of electrons in 3 mm of silicon corresponds to approximately 1600 keV, there should be a high probability of complete absorption of all incident electrons of lesser energy in the small silicon detector. On the other hand, higher-energy electrons will be incompletely absorbed. [Notice how this influences the Fermi plot of In^{114m} ($E_{max}=1984$ keV) in Fig. 4.] If we use this detector only for the study of the lower-energy portion of the spectrum only the backscattering correction outlined above need be applied. In the study of the higher-energy portion of the spectrum we used the large silicon detector with the electrons incident upon one of the 5-mm by 12-mm faces of the detector. The 12-mm thickness of silicon corresponds to the range of 5.3-MeV electrons. Thus while it is possible to absorb in this detector the full energy of higher-energy electrons, there is an appreciable probability not only for backscattering, but also for an electron incident upon the 5-mm by 12-mm face to escape through one

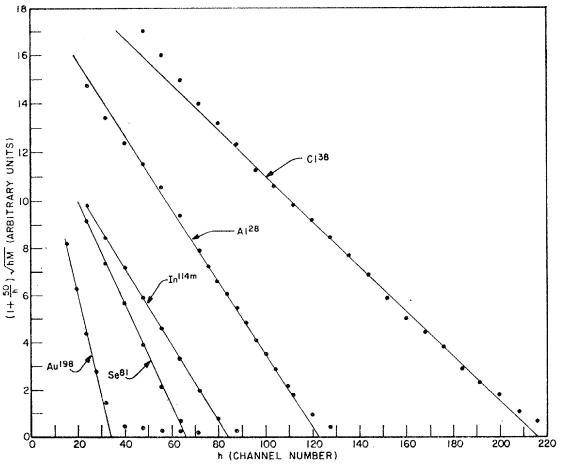

FIG. 5. Fermi plots of the β-ray spectra of Au^{198}, Se^{81}, In^{114m}, Al^{28}, and Cl^{38}; from data recorded with the large lithium-drifted silicon detector.

[24] M. S. Freedman, T. B. Novey, F. T. Porter, and F. Wagner, Jr., Rev. Sci. Instr. **27**, 716 (1956).
[25] G. Bertolini, F. Cappellani, and A. Rota, Nucl. Instr. Methods **9**, 107 (1960).

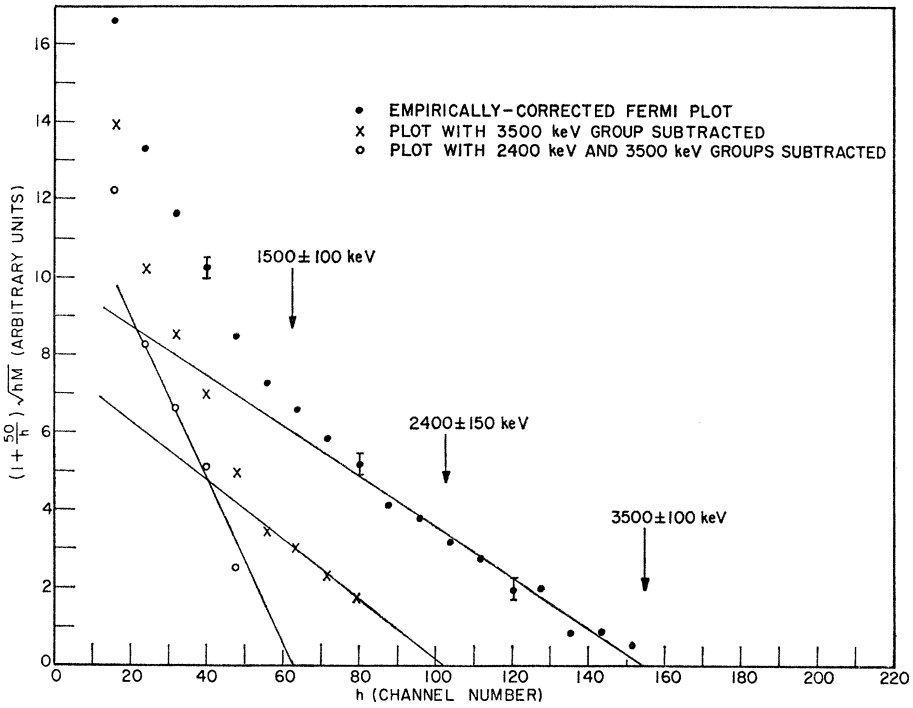

FIG. 6. Fermi plot of the β-ray spectrum of the short-lived isomer of Se^{83} from data recorded with the large lithium-drifted silicon detector.

of the 12-mm by 12-mm faces after depositing only part of its energy in the detector. For the particular experimental conditions used, we found empirically that $[1+(50/h)](hM)^{1/2}$ versus h would give reasonably straight Fermi plots for β-ray transitions with widely differing end-point energies, where $M(h)$ is the measured spectrum. Figure 5 shows the analysis of the β-ray transitions with end points at 962 keV (Au^{198}), 1560 keV (Se^{81}), 1984 keV (In^{114m}), 2868 keV (Al^{28}), and 4810 keV (Cl^{38}). Not all of the data points are shown, but those presented are sufficient to show that the desired straight-line representation is remarkably good for such a crude analysis.

B. β-Ray Spectra of Se^{83}

1. The Short-Lived Isomer

A sample of the enriched selenium was mounted in thin polyethylene film, irradiated for 2 min in the pneumatic rabbit facility of the nuclear reactor, and following a 1.5-min waiting period, was counted for 2 min with the larger silicon detector. This cycle was repeated until statistically significant data were accumulated. The empirically corrected Fermi analysis of the data is shown in Fig. 6. The data in groups of seven channels were averaged before analysis, in order to reduce statistical scatter as well as analysis time. Expected statistical deviations are shown for a few representative points. The highest-energy component, and then the next-highest-energy component were subtracted out with the results shown on the figure. Although no error flags are indicated on the plots of the remaining components, the errors are larger (by a factor of approximately 1.5). Indicated on Fig. 6 is the energy (with estimated error) for the three observed β-ray transitions, 1500±100 keV, 2400±150 keV, and 3500±100 keV. While a fuller discussion will be deferred to a later section, it may be observed here that these results are not in serious disagreement with (and are perhaps less accurate than) those of Cochran and Pratt[12,13] for the 70-sec isomer of Se^{83}.

2. The Long-Lived Isomer

For measurements on the long-lived isomer, the same procedure described above was used, except that the selenium was irradiated with 10-times higher neutron flux, and the counting cycle was changed to 3-min neutron irradiation, 9-min wait, and 40-min count. The accumulated data from the large silicon detector were analyzed as before with the results shown in Fig. 7. Impurities were found to be present in the sample and sample holder, and independent measurements of γ radiation with NaI(Tl) and germanium detectors confirm the assignments of the 4900±100-keV β-ray transition to Cl^{38} and the 2880±150-keV β-ray transition to Al^{28}.

The smaller silicon detector was used with the same counting routine as above to observe the low-energy β-ray transitions. The resulting data were corrected for backscattering and subjected to Fermi analysis. Only allowed transitions were considered in the analysis since the quality of the data could not justify the refinement to consideration of forbidden transitions. A typical

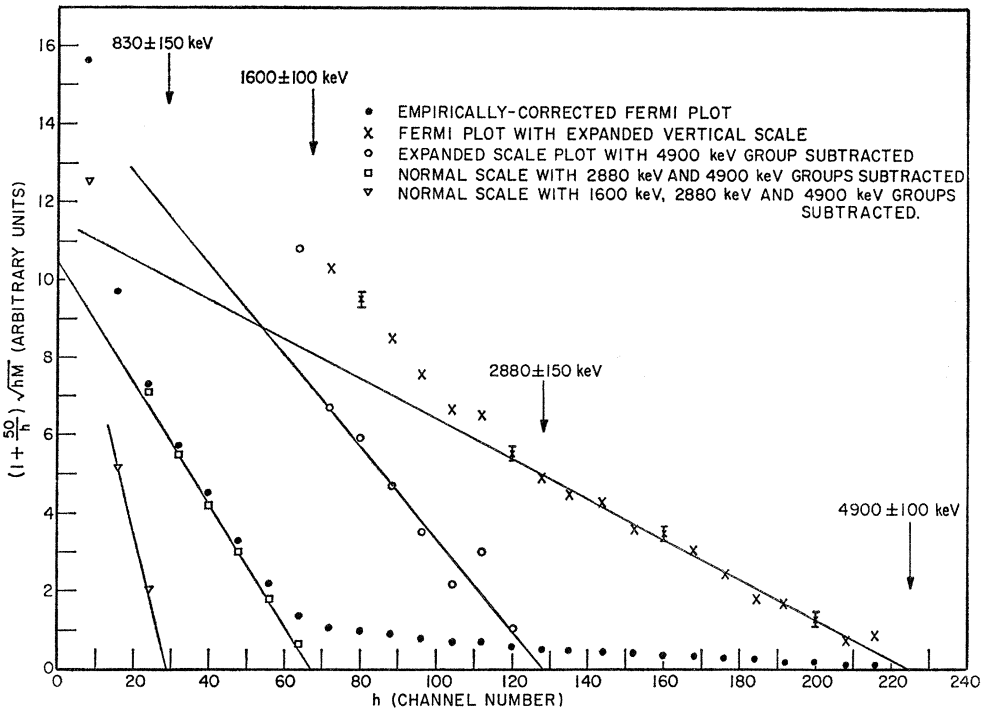

FIG. 7. Fermi plot of the β-ray spectrum of the long-lived isomer of Se^{83} from data recorded with the large lithium-drifted silicon detector.

result is shown in Fig. 8. The high-energy contribution, which is fortunately relatively small, was subtracted out as a single β-ray group although we know from Fig. 7 that it is not a single group. Only two β-ray groups are observed to remain. The 1560-keV transition agrees very well in energy with that observed in Se^{81} by Kuroyanagi.[26] For comparison, samples of selenium enriched to 94.4% in Se^{80} were activated to observe the β-ray spectrum of Se^{81}. The analysis of the Se^{81} β-ray spectrum showed essentially one component of 1560 keV, confirming the value obtained by Kuroyanagi. We will show by means of β-γ coincidence measurements reported in Sec. VII, however, that at least part of the observed intensity of the 1560-keV group is due to Se^{83}. Figure 8 indicates only one remaining β-ray group (above 300 keV) with energy 920 keV. We will show in subsequent portions of this paper, however, that several β-ray groups occur in the decay of Se^{83}. Those results show that not only are a number of transitions with approximately the same energy responsible for the observed 920-keV β-ray group, but also that higher-energy transitions occur with much lower intensity. We have been unable to reach such conclusions from the experimental work reported in this section, due to the combined effects of energy resolution and γ-ray sensitivity of the detector and the continuous character of β-ray spectra. Therefore, we shall defer further discussion of the results of the present section to Secs. VII and XI so that all results may be discussed together.

VI. γ-RAY COINCIDENCE SPECTRA

A. Experimental Apparatus

Coincidence spectra were recorded, using the germanium detector described in Sec. IV as the analyzing detector and a 4.5-cm-diam by 5.1-cm-long NaI(Tl) scintillation crystal mounted on a type 6810-A photomultiplier served as the gating detector. Conventional electronics were used for energy selection and coincidence timing. A previously described gain-stabilization system[27] was used in conjunction with the scintillation detector. The coincidence circuit was operated in the fast-slow mode with the coincidence resolving time

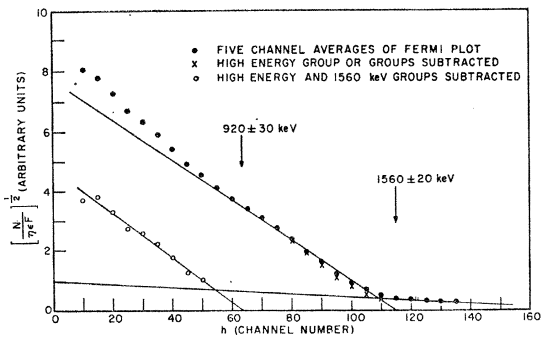

FIG. 8. Fermi plot of the β ray spectrum of the long-lived isomer of Se^{83}, from data recorded with the small lithium-drifted silicon detector.

[26] T. Kuroyanagi, J. Phys. Soc. Japan 15, 2179 (1960).

[27] K. W. Marlow, Nucl. Instr. Methods 15, 188 (1962).

TABLE III. Coincidence relative intensities of γ rays accompanying the decay of the long-lived isomer of Se^{83}.

γ-ray energy (keV) \ Gating channel (keV)	320–400	460–540	690–750	770–830	830–930	1275–1375
226	39 ±2	35.0±0.6	15.0±0.5	14.0±0.4	12.0±0.3	10.0±0.9
261		0.3±0.2				0.3±0.1
296						0.4±0.2
356	22 ±1	58.0±0.6	24.0±0.5	20.0±0.6	15.0±0.3	43.0±0.9
387						3.0±0.4
416		1.6±0.2	0.8±0.2	0.4±0.1		1.3±0.4
457	2.5±0.2	2.0±0.3	1.3±0.2	1.8±0.2	2.4±0.3	2.4±0.8
487	2.2±0.9	2.0±0.3	<0.6	<0.6	<0.3	1.4±0.4
512	58 ±2	17.0±0.9	17.0±0.5	16 ±1	11.0±0.3	21 ±1
554	2.8±0.9	1.9±0.3	0.9±0.2	2.2±0.4	1.7±0.3	7.3±1.0
572	3.7±0.9	4.2±0.3	0.4±0.2	1.2±0.4	1.5±0.2	6.4±1.0
601						1.2±0.4
610	3.9±0.9	3.7±0.3				
636			0.8±0.2			
666	4.3±0.9	1.2±0.5	2.4±0.5		1.5±0.5	
720	24.0±0.9	20.0±0.8	4.3±1.2	4.4±0.4	7.4±0.5	
801	4.6±0.6	6.4±0.6	2.5±0.5	2.4±0.6	2.6±0.5	11.0±1.5
837	14.0±0.7	14.0±1.2	7.2±0.7	7.2±0.4	2.3±0.6	0.7±0.6
868		1.6±1.2	4.3±1.0	4.0±1.0	2.6±0.6	1.9±0.8
874		4.8±1.7				
886	11.0±1.2	9.9±1.7	4.3±1.0	6.8±1.0	2.7±0.6	0.8±0.6
997						2.5±0.8
1065	4.7±0.9				0.6 ±0.3	9.0±1.6
1082	2.7±1.3					6.9±1.6
1129						2.2±1.2
1183					1.1±0.5	
1192	5.3±1.2	6.4±1.7	1.8±0.6	<0.2	1.4±0.5	1.8±0.8
1205		1.0±0.5				
1270	13.0±1.8	7.5±1.2				
1299	9.9±1.8	7.5±1.2	0.6±0.3		1.0±0.3	3.0±1.2
1308	3.4±3.0					
1319	10 ±3	4.4±1.2	0.6±0.3			
1344	2.9±1.0	5.8±1.5		1 ±1	0.8±0.3	4.7±1.6
1355	1.7±0.8	3.1±1.2			0.7±0.3	6.5±1.6
1397	2.0±0.6					
1421						4.7±1.6
1558	1.8±0.9	1.7±1.2				
1784		2.6±0.9				
1897			1.8±0.6	7.8±1.0	3.6±0.8	
1969		0.4±0.2				
2046		0.6±0.2				
2291	10.4±1.2					
2338	5.0±0.9					
2421	2.9±1.4					

(2τ) set at 70 nsec. The output of the coincidence circuit was used to open the coincidence gate of the 512-channel pulse-height analyzer. The two detectors formed a 90° angle with the source at the vertex, each detector being 1.5 cm from the source. A 9-mm Lucite β-ray shield was interposed between each detector and the source, and a 5-mm thick Pb shield covered with 1 mm of Sn was placed between the two detectors to help prevent the detection of false coincidences due to scattered γ rays.

Sum-coincidence spectra[28] as well as ordinary coincidence spectra were recorded with 4.5-cm-diam by 5.1-cm-long NaI(Tl) scintillation crystals. The NaI(Tl) crystals were mounted on type 6810-A photomultipliers. Fast signals for coincidence timing were obtained from the anodes, while energy-dependent signals were obtained from the eighth dynodes. For the fast-slow coincidence system,[29] the coincidence resolving time (2τ) was dependent on the length of the shaped anode signals and, in this case, was 35 nsec. Both detectors were gain-stabilized.[27]

B. Germanium Detector Coincidence Spectra

Using the germanium coincidence spectrometer described above, coincidence γ-ray spectra were recorded for the decay of the long-lived isomer of Se^{83}. Figures 9 and 10 show coincidence spectra for selected energy regions of 320 to 400 keV and 460 to 540 keV, respectively, in the gating detector. Each full absorption peak was corrected for the relative efficiency of the germanium detector as in Sec. IV to deduce the relative intensities of the gamma rays in each coincidence

[28] A. M. Hoogenboom, Nucl. Instr. Methods 3, 57 (1958).

[29] K. W. Marlow (to be published).

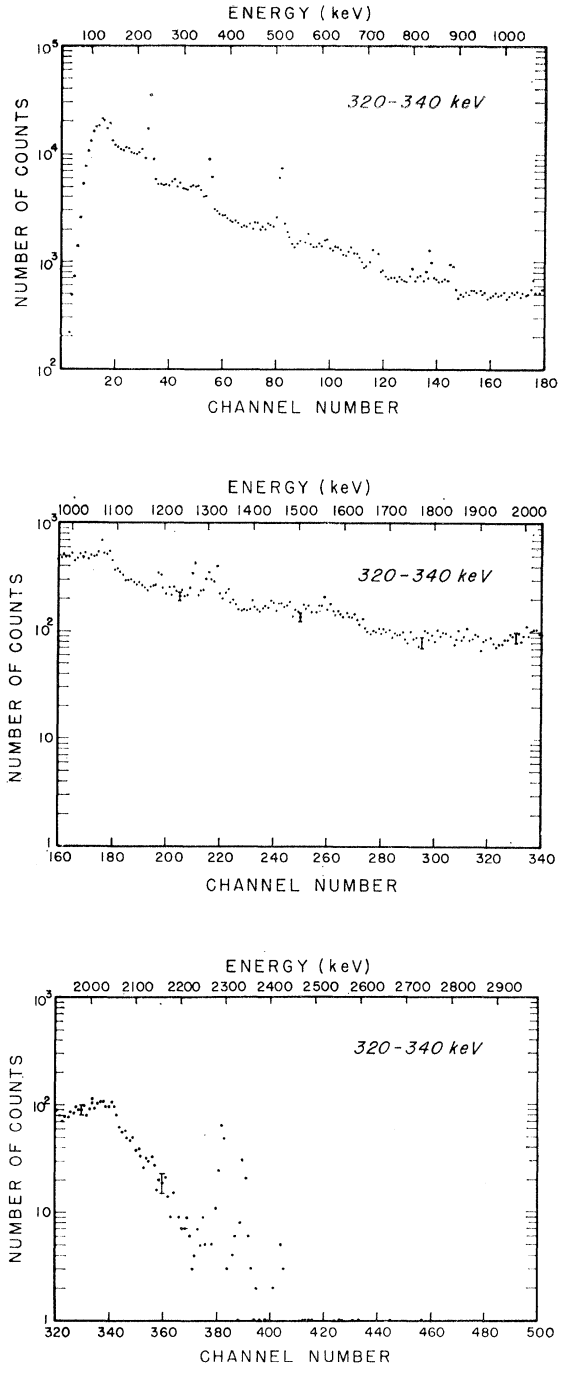

FIG. 9. Germanium detector coincidence γ-ray spectrum for the decay of the long-lived isomer of Se^{83}. The selected energy region for the NaI(Tl) gating detector is given on the figure.

spectrum. In addition to the data shown in Figs. 9 and 10, other coincidence spectra were recorded with the gating channel covering the following energy regions: 690 to 750 keV, 770 to 830 keV, 830 to 930 keV, and 1275 to 1375 keV. The relative intensities deduced from these spectra are listed in Table III. Peaks at 1145, 1645, 2170 and 1724 keV (due to Cl^{38} and Na^{24} contaminants) were not included. An estimated error of 2 keV has been assigned to the γ-ray energies.

Although most of the strong coincidence relationships may be easily obtained from this data, four important points must be kept in mind when considering the *weaker* relationships. The first point is that no corrections have been made for the double-escape effect due

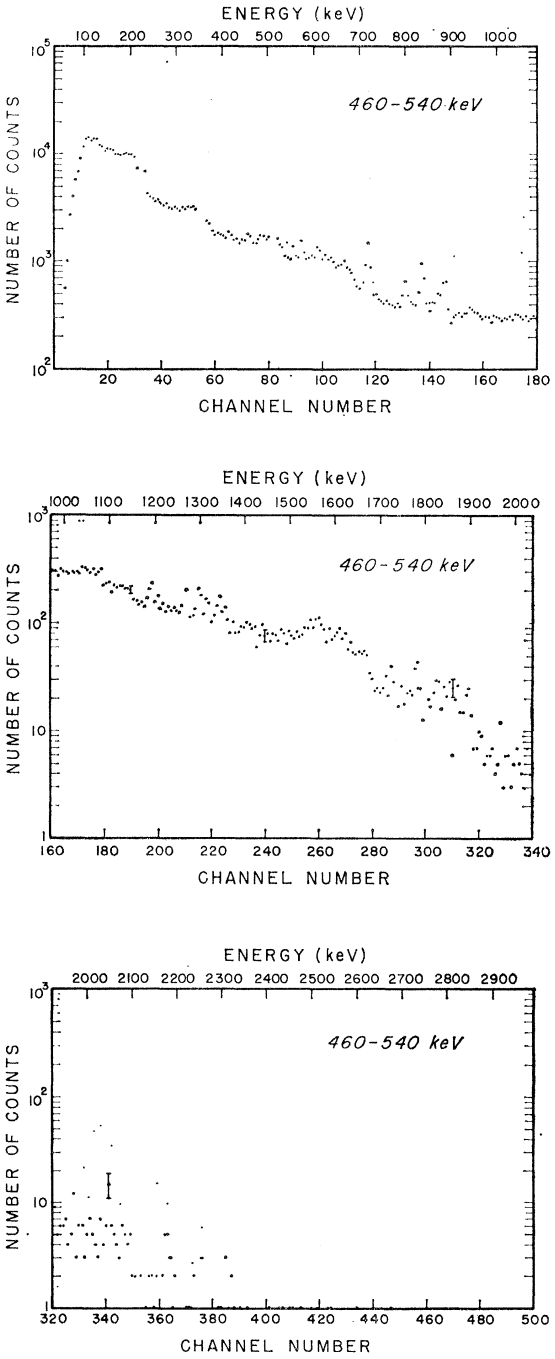

FIG. 10. Germanium detector coincidence γ-ray spectrum for the decay of the long-lived isomer of Se^{83}. The selected energy region for the NaI(Tl) gating detector is given on the figure.

to pair production resulting from high-energy γ rays. Secondly, the values of, and the relative errors on, the relative intensities given in Table III may only be compared in detail for values within a given column. The third point is that some low-intensity γ rays, which might otherwise be noticed in a given spectrum, could be obscured by the Compton distribution of higher-energy γ rays. This last point is most important where the high-energy γ rays in coincidence with the 356-keV γ rays may obscure lower-intensity, lower-energy γ rays in the same spectrum. The final point that should be made regarding the low-intensity γ ray is that since some sets of the data were more statistically valid than others the absence of relative intensity notations in some parts of Table III may be only an indication that peaks could not be differentiated from statistical deviations in the data points of a spectrum.

In interpreting the *stronger* relationships in Table III, it is important to observe that most of the energy regions selected by the gating detector include the effect of more than one photopeak.

While a more encompassing discussion of experimental results will be presented in Sec. XI, certain major conclusions will be drawn from the coincidence results at this point in order to clarify some of the experiments and their results which will be reported in intervening sections.

We first observe that the 356-keV γ ray is probably a transition to the ground state since it is the only intense γ ray in the decay of both isomers of Se^{83} (see Tables I and II). This suggestion is reinforced by the observation that it is the only γ ray in coincidence with the high-energy 2291- and 2338-keV γ rays (see Table III), as well as the fact that it is the most intense γ ray in any of the coincidence spectra (see Table III). Further proof for this contention can be found from energy and intensity balance considerations, and by the delayed-coincidence measurements reported in Sec. VIII.

We next observe that the relatively intense γ rays observed in the singles data at 226, 512, 720, and 837 keV have an energy sum of 2295 ± 4 keV, which agrees well with the value for the 2291 ± 2 keV γ ray. Further, the γ rays at 226, 512, 720, and 886 keV have an energy sum of 2344 ± 4 keV which is in agreement with the value for the 2338 ± 2-keV γ ray. This suggests that 2291- and 2338-keV γ rays are cross over transitions of four-step cascades which differ only in the first step. The coincidence intensities reported in Table III confirm that the 356-, 512-, 226-, and 720-keV γ rays are each in coincidence with one another and with the 837- and 886-keV γ rays, whereas the 2291- and 2338-keV γ rays are coincident only with the 356-keV γ ray. Since no other γ rays have been observed which would add a sixth step in either of the five-member γ-ray cascades, we propose that there exists an excited level at 2650 keV for which the principal modes of decay are by either 837- or 2291-keV γ-ray transitions to levels at 1814 and 356 keV, respectively. Similarly there is an excited level at 2697 keV which decays principally by 886- or 2338-keV γ-ray transitions to the 1814- and 356-keV levels.

To establish the excitation energy of other levels, it is of interest to determine the order of the 226-, 512-, and 720-keV γ-ray cascade connecting the 1814- and 356-keV levels. It is fairly easy to place the 512-keV γ ray in the sequence. (The possibility that the 512-keV γ ray should be identified as an anihilation photon has been ruled out by an experiment reported in Sec. IX.) Energy and intensity balance considerations (using the "singles" data from Table I and coincidence data from Table III) show that a level exists at 868 keV, which can decay either to the 356-keV level or to the ground level.

Although a study of the coincidence intensities leads to the same conclusion, delayed-coincidence measurements reported in Sec. VIII provide a direct measurement showing that the 356-, 512-, and 226-keV γ rays follow the 720-keV γ ray. Therefore, a level exists at 1094 keV.

Summarizing the conclusions which have been drawn from the data at this point, the excitation energies of levels in Br^{83} which are strongly populated by the long-lived Se^{83} decay are: 356 ± 2, 868 ± 2, 1094 ± 3, 1814 ± 3, 2650 ± 4, and 2697 ± 4 keV.

C. Scintillation Detector Coincidence γ-Ray Spectra

1. Sum-Coincidence Spectra

The NaI(Tl) scintillation detectors were used to record sum-coincidence spectra.[28] In general agreement with Ythier and van Lieshout,[14] we have observed a prominent sum peak in the spectrum obtained with a NaI(Tl) well crystal, indicating that there was strong β-ray feeding to one or more levels at approximately 2660 keV in the Br^{83} nucleus. Accordingly, sum-coincidence spectra were recorded with the sum channel corresponding to approximately 2660 keV in order to reveal which pairs of γ rays were in cascade from that level.

The two NaI(Tl) detectors used in the spectrometer were placed directly opposite each other with 1.2-cm separation between the crystal faces. Each detector face was covered with 0.5-mm each of Al, Sn, Ta, and Pb. Two 6-mm-thick Pb "backscatter" shields (covered by 0.2 mm each of Sn and Cu) were placed in line between the two detectors so that there was between their edges a gap of approximately 3 mm in which the source was placed.

Due to the nonlinear relation between pulse height and energy for the NaI(Tl) scintillation detectors, the height of the sum-pulse due to coincident radiations is not linearly related to the sum of the energies of the radiations. This situation exists whether the coincident

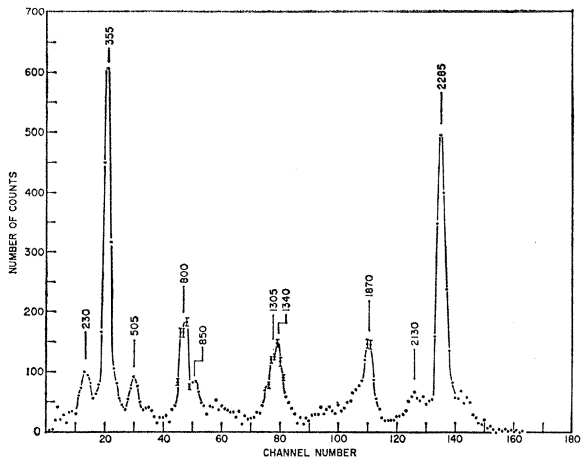

FIG. 11. Sum coincidence γ-ray spectrum of the decay of the long-lived isomer of Se^{83} for a 30-keV sum channel centered at 2660 keV.

radiations are absorbed in one scintillation crystal, or the electronic signals being added are due to coincident radiations absorbed in two separate scintillation crystals.[30] Because of the nonlinear relation, the sum-channel setting was calibrated with the sums of well-known coincident radiations.

A 30-keV-wide sum channel was set so that its center corresponded to a 2660-keV sum and the energy-dependent signal of one of the detectors satisfying the sum condition was analyzed in the 512-channel pulse-height analyzer, resulting in the spectrum shown in Fig. 11 for the long-lived isomer of Se^{83}. It was found that contaminating Na^{24} activity could contribute to the spectrum of Fig. 11 at most only part of the peak near 1300 keV. Using the equations given by Naqvi[31] for the efficiency of a sum-coincidence spectrometer, the relative intensity of the different cascades were deduced. These results are shown in Table IV. The intensity is normalized to 100 for the "2300–355" keV cascade, and the estimated errors are based only on counting statistics. It should be pointed out that, at the time these data were taken, there was thought to be only one "2300-keV" γ ray and no other levels close to the "2600-keV" level. Since there are additional levels within approximately 100 keV of 2660 keV, the chosen sum condition includes transtions from those levels. We have studied the distortion of sum spectra for nonideal sum-channel settings and conclude that the "800–1870 keV" cascade noted in Fig. 11 is a cascade of the 801- and 1897-keV γ rays which were observed with the lithium-drifted germanium detector.

TABLE IV. Relative intensity of cascades in Br^{83} deduced from the sum-coincidence spectra.

Gamma rays (keV)	Intensity
355, 2300	100±2
800, 1870	51±2
850, 1790	13±2
1330, 1330	16±2

[30] J. Kantele and R. W. Fink, Nucl. Instr. Methods **13**, 141 (1961).
[31] S. I. H. Naqvi, Nucl. Instr. Methods **16**, 305 (1962).

Other measurements were made on the decay of Se^{83} with various sum channel settings, both below and above 2660 keV, and with the axes of the detectors forming a 90° angle. No new or contradictory information was derived from these experiments.

2. *Scintillation-Coincidence Spectra*

The scintillation detectors were also used to record the γ-ray spectrum measured by one detector in coincidence with the γ rays being detected in a certain selected energy range in the other detector. In all of these experiments the detectors were placed with their axes at a 90° angle and the face of each crystal was 4 cm from the source. Pb absorbers were used to prevent scattering of γ rays from one detector to the other. For most of the experiments, the front face of each detector was covered by 0.5 mm each of Al, Sn, Ta, and Pb in order to suppress the detection of scattered radiation.

Because of the poor energy resolution of NaI(Tl) detectors, it was not always possible to tell whether or not a given peak was complex. Coincidence experiments using the germanium detector removed much of the energy-resolution difficulty. However, the many scintillation coincidence spectra obtained before the germanium detector became available are of interest in a qualitative way as an aid in interpreting the germanium coincidence spectra, and in showing coincidence relationships where the gating detector was used to select higher-energy regions than were used in measurements with the germanium detector. In particular, Fig. 12 helps to confirm the coincidence of the 801- and 1897-keV γ rays.

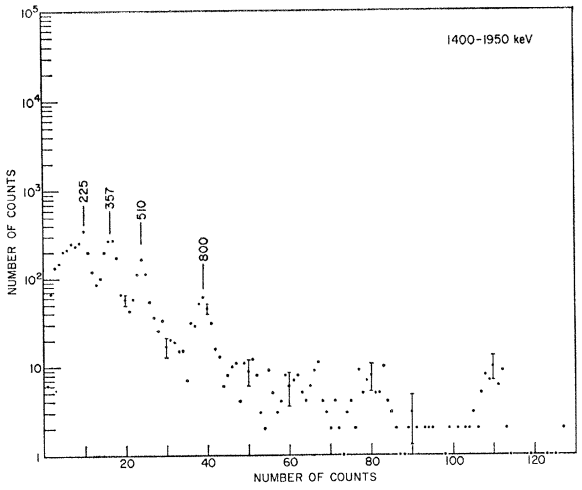

FIG. 12. Scintillation coincidence γ-ray spectrum for the decay of the long-lived isomer of Se^{83}.

D. Coincident Summing of the γ Rays from 70-sec Se^{83m} in the Total-Absorption Spectrometer

A 7.6-cm-diam by 7.6-cm-long cylinder of NaI(Tl), with a 0.95-cm-diam by 4.5-cm-deep axial "well," was mounted on a type 8054 photomultiplier. This detector was used to record γ-ray spectra with a radioactive source inside the well so that coincident γ rays were represented as their sum. The detector system was also gain-stabilized.[27] While counting, the source was covered with 1 mm of Sn to absorb β rays and some of the low-energy γ rays of Se^{75}, Se^{77}, and Se^{79}.

The enriched selenium sample was activated, allowed to decay for two minutes, counted inside the well counter for two minutes in the "add" mode of the pulse-height analyzer, allowed to decay for one more minute, and then counted in the "subtract" mode for 2 min. This procedure was repeated with different samples until sufficient data were accumulated. The resultant spectrum (Fig. 13) shows peaks corresponding to 160 (Se^{77}), 360, 670, 1030, and 2050 keV. An oversubtraction caused a distortion in the 270- and 400-keV regions. This may provide some evidence either for an isomeric activity in Se^{75}, or for production of Ge^{75} activity by the reaction $Se^{78}(n,\alpha)Ge^{75}$. The peak at 1030 keV is definitely wider than that due to a γ ray of a single energy, indicating the presence of the 989- and 1063-keV γ rays and/or sum peaks. The peak at 2050 keV also appears to be complex, which may be an indication of other levels in the region of 2000 keV. Of greater importance, however, was a notable absence of sum peaks corresponding to levels between 1100 and 1900 keV and above 2200 keV. This result precludes certain placements in the decay scheme of some of the prominent gamma rays of the 70-sec activity. The consequences of these results will be discussed in Sec. XI.

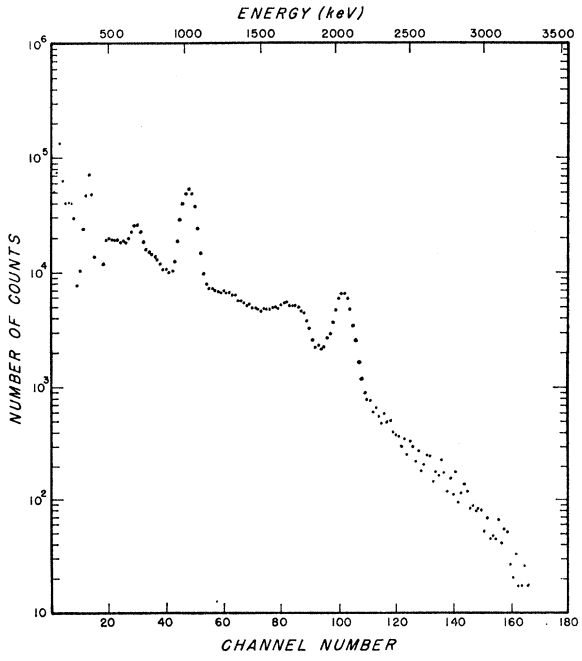

FIG. 13. γ-ray spectrum of the short-lived isomer of Se^{83}, recorded with the source inside the well of the scintillation spectrometer.

VII. β-γ COINCIDENCE MEASUREMENTS

The scintillation γ-ray detectors and the silicon β-ray detectors already discussed were used for detection of γ rays in coincidence with β rays. Since the charge collection time in the silicon detectors varied, depending upon where the incident electrons were absorbed, a coincidence resolving time of 120 nsec was used in order to assure 100% coincidence efficiency at all electron energies.

The larger silicon detector (discussed in Sec. V) was used for measurements of high-energy β rays. Since we have already observed in Secs. IV and V that the principal β decay is to one or more levels near 2660 keV, it was considered of interest to investigate the existence of higher-energy β rays to lower-lying levels in Br^{83}. The 226-, 356-, and 512-keV γ rays have been shown, from the γ-ray coincidence results of Sec. VI and the delayed-coincidence measurements described in Sec. VIII, to be transitions in the lower part of the decay scheme. Therefore the energy-selection channel for the γ-ray detector was set for the region 180–550 keV to include the photopeaks from all three γ rays. The resultant coincidence β-ray spectrum was analyzed as in the singles data (Sec. V) and the resultant Fermi plot is shown in Fig. 14. It is interesting to note that Baskova *et al.*[15] observed a β-ray transition of 3300 keV but did not find it in coincidence with any γ ray. While this 3200-keV β-ray transition was obscured in the singles spectrum by the effect of impurities, it remains a weak contribution even in the coincidence spectrum. The presence of the "900"-keV β-ray transition is not surprising, but the "1500"-keV transition was somewhat unexpected because of the interpretation (in Sec. V) that all of the 1560-keV transition in the singles data might be due to Se^{81}. Since the 1560-keV β-ray transition in Se^{81} has not been found to be in coincidence with γ rays,[26] we conclude that at least part of the observed singles intensity of the "1500"-keV transition is due to Se^{83}.

The lower-energy β-ray transitions were further investigated with the smaller silicon detector in the coincidence spectrometer. β-ray spectra in coincidence with γ rays in the energy range 200–540 keV and in coincidence with γ rays with energy greater than 540 keV were recorded. These data were analyzed as before (Sec. V) and the results are presented in Figs. 15 and 16, respectively. Figure 15 shows that the low-energy β-ray data is more complicated than would have been expected from the data shown in Fig. 14. The high-energy groups shown in Figs. 15 and 16 have not been assigned an energy because of the experimental difficulty with high-energy electrons demonstrated by the In^{114m}

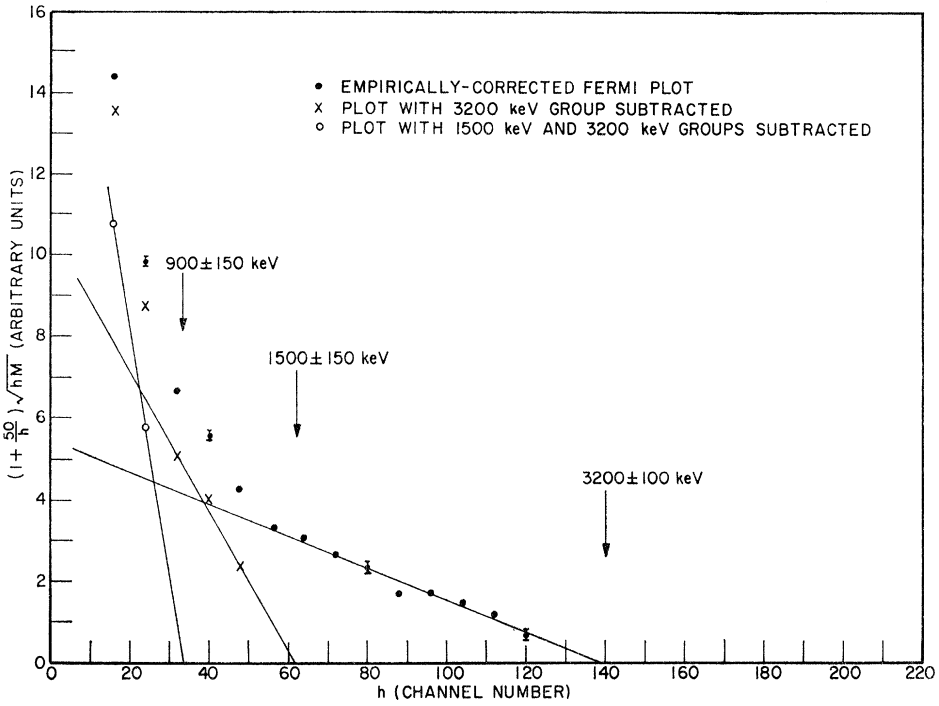

FIG. 14. Fermi plot of the coincidence β-ray spectrum of the long-lived isomer of Se^{83}, with the gating channel including γ rays in the energy region 180 to 550 keV (large silicon β-ray detector).

spectrum in Fig. 4 and because the high-energy groups were studied by the large detector whose results are shown in Fig. 14.

The 940-, 1510-, and 3200-keV groups are surely due to Se^{83}, while the remaining β groups observed in Fig. 15 are consistent with the results of Kuroyanagi[26] for Se^{81}.

The weighted mean of four singles measurements (Sec. V) and four coincidence measurements (this section) resulted in 930±40 keV for the end point energy of the principal β-ray transitions of the long-lived isomer of Se^{83}.

VIII. DELAYED COINCIDENCE MEASUREMENTS

A. Determination of the Lifetime of the Delayed Level in Br^{83}

To determine the temporal order of certain γ rays and the lifetime of excited levels in Br^{83}, delayed coincidence measurements were performed with a transistorized time-to-pulse-height converter (TPHC).

The calibration showed the TPHC to have a linear relation between pulse height and time over a range of at least 80 nsec. For most of the lifetime measurements a conversion ratio of 0.85 nsec/channel was used. The detectors used in this measurement were the same as those used in the scintillation γ-ray coincidence spectrometer. They were placed 4 cm from the source, their axes forming a 90° angle with the radioactive source at its vertex, and lead shielding prevented scattering from one detector to the other. Time spectra were recorded for the photopeak region of many of the γ rays observed in the γ-ray spectra. In some cases the Compton distribution from higher-energy γ rays caused some interference, but in general the results are unambiguous.

Results, such as those shown in Fig. 17A, using start/stop energy bands of 460–550 keV/320–410 keV, 200–240 keV/490–530 keV, and 200–240 keV/320–390 keV show that the 226-, 356-, and 512-keV γ rays are in "prompt" coincidence with one another (i.e., the delay is too short to measure with the equipment being used). Figure 17B shows that at least one of these three γ rays follows in time one or more γ rays with energy in the 550–880-keV region. Figure 17C not only demonstrates the reversal obtained when the start-stop function of the energy-selected regions are interchanged, but also shows that some of the γ rays feeding the delayed level exceed 900 keV. It further indicates that the 226-keV γ ray follows the delayed level. The delayed contributions in Figs. 17D and 17E show that the 356- and 512-keV γ rays also follow the delayed level. A prompt distribution was obtained with start/stop bands of 410–460 keV/670–900 keV, representing an energy region selected between the photopeaks of the 356- and 512-keV γ rays, and demonstrates that the energy selection for these two γ rays is not adversely affected by higher-energy γ rays. The fact that there is a significant contribution of prompt coincidences in the 356- and 512-keV data indicates that the levels which these γ rays de-excite are fed by transitions from both prompt and delayed levels. Figure 17F, however, showing the 226-keV γ ray delayed with respect to the 720-keV γ ray, has a time distribution which may be explained as

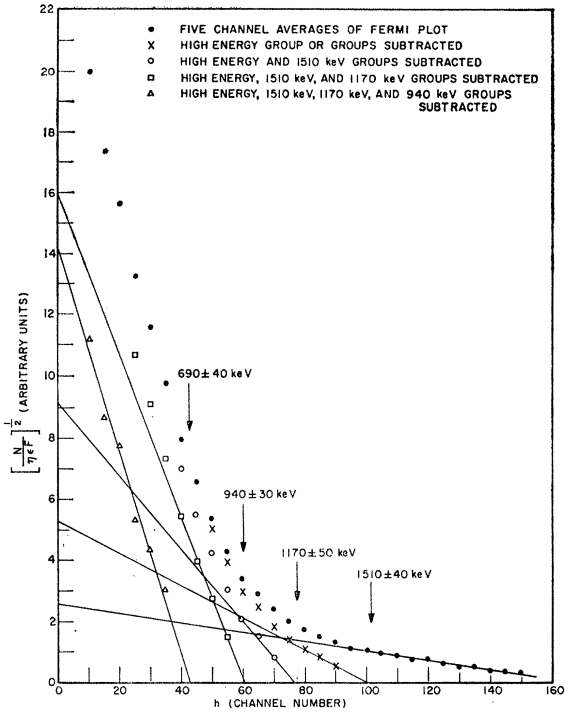

FIG. 15. Fermi plot of the coincidence β-ray spectrum of the long-lived isomer of Se^{83}, with the gating channel including γ rays in the energy region 200 to 540 keV (small silicon β-ray detector).

entirely due to delayed coincidences. This result, coupled with the previously described results, shows that the delayed level decays by the emission of the 226-keV γ ray followed by the 512- and 356-keV γ rays. The delayed level is populated by the 720-keV and higher-energy γ rays. These conclusions are in full agreement with those of Sec. VI.

As a check on the possibility of the delayed level being due to the presence of Se^{81} activity, an experiment was performed using the samples enriched in Se^{80}. The principal coincidences are due to "270"-keV γ rays in coincidence with "270"- and "550"-keV γ rays. The data from start/stop energy bands of 200–300 keV/220–700 keV could not be distinguished from a prompt distribution, so one must conclude that the delayed level cannot be due to the decay of Se^{81}.

The exponential decay of the delayed distributions were all observed to correspond to a half-life of approximately 4 nsec. In order to obtain a more precise measure of the half-life, further measurements were made on the 720–226 keV cascade (as in Fig. 17F) and a section of the delayed portion of the spectrum was fitted to an exponential function by the method of least squares. The data used for the fit extended over 5 half-lives. The result of the least-squares determination gave $T_{1/2}=4.08\pm0.03$ nsec. After considering the various sources of errors, principally in the time calibration, a final result of $T_{1/2}=4.1\pm0.1$ nsec is obtained for the delayed level in Br^{83}.

B. Spectrum of the γ-Rays Populating the Delayed Level in Br^{83}

To obtain further information about which γ rays were populating the delayed level, a TPHC was designed, following the suggestion of Weisberg and Berko,[32] which did not give an output pulse unless the start and stop pulses coincided within a specified time interval. With this change made, the scintillation γ-ray spectrum in coincidence with γ rays in a selected energy region was sorted into different spectra corresponding to different coincidence delays.

Figures 18(a), 18(b), and 18(c) show the accidental, prompt, and delayed coincidence spectra, respectively, for the 512-keV γ ray. These are an accumulation of data taken on four different days. The data on the individual days were inspected separately and were found to be consistent with the summed data. The prompt channel selected events in time extending from -4 to $+2$ nsec, with time measured from the peak of a prompt distribution; the delayed channel selected events extending in time from $+14$ to $+22$ nsec; and

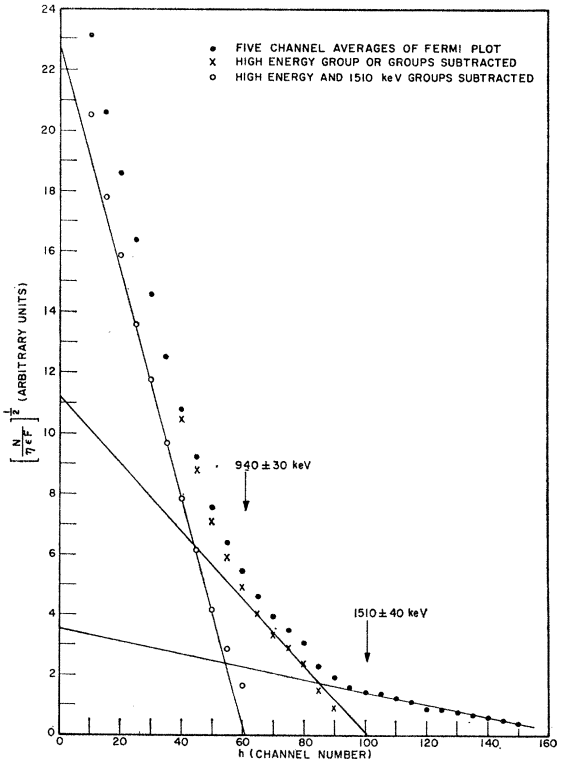

FIG. 16. Fermi plot of the coincidence β-ray spectrum of the long-lived isomer of Se^{83} with the gating channel including γ rays greater than 540 keV (small silicon β-ray detector).

[32] H. L. Weisberg and S. Berko, IEEE Trans. Nucl. Sci. **11**, 406 (1964).

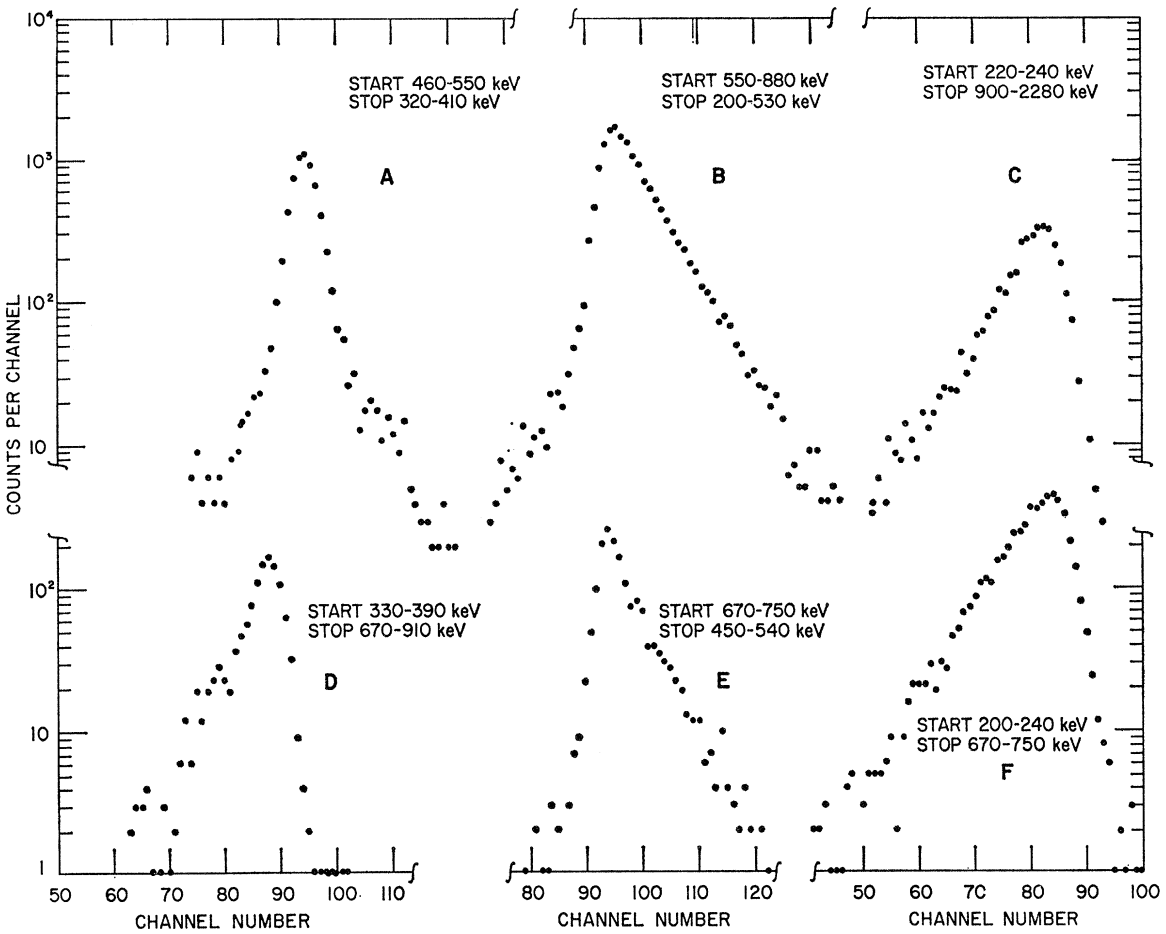

FIG. 17. Time spectra of γ rays observed in the decay of the long-lived isomer of Se^{83}.

the accidental channel from -35 to -22 nsec. The data shown in Fig. 18 indicate that the 720- and 837-keV γ rays are the main feeders of the delayed level. The distortion of the high-energy side of the 837-keV peak in Fig. 18(c) indicates a contribution due to a peak in the region from 850 to 900 keV which, considering the germanium detector results reported in Sec. VI, must be the 886-keV γ ray. Other higher-energy γ rays of lower intensity apparently contribute to the feeding of the delayed level, but cannot be resolved in these data. The low-energy γ-ray peaks occurring in the delayed spectrum can be entirely accounted for as accidental coincidences.

Accidental, prompt and delayed coincidence spectra were also obtained for the 356-keV γ ray and while a fewer number of counts were accumulated (because of a shorter counting time), the delayed-coincidence results were in complete agreement with those for 512 keV. The prompt-coincidence results differed somewhat (as expected from the coincidence spectra reported in Sec. VI) in that the 356-keV data showed extra peaks (principally at 1065, $\approx$1270, and 2300 keV).

IX. LIFETIME OF THE LONG-LIVED ISOMER OF Se^{83}

Three measurements of the lifetime of the long-lived isomer of Se^{83} were made. Each of these involved following the time dependence of the γ radiation from the Se^{83} source for about 24 h. (A counting cycle of 100 sec—90 on, 10 off—was used in each case.) They differed in the preparation of the source and the requirements placed on the γ rays.

A. The Chemically Separated Sample

A sample of the selenium enriched in Se^{82} was irradiated and then chemically cleaned before counting in order to eliminate the possibility that the principal activity could be due to germanium or arsenic isotopes produced by the (n,α) or (n,p) reactions and in order to remove undesirable activities such as Cl^{38}. The entire chemical separation procedure (including transportation) took 45 min. The chemical separation procedure was not oriented particularly to sodium removal, so that there remained an appreciable quantity of Na^{24} activity from treatment of the selenium sample before

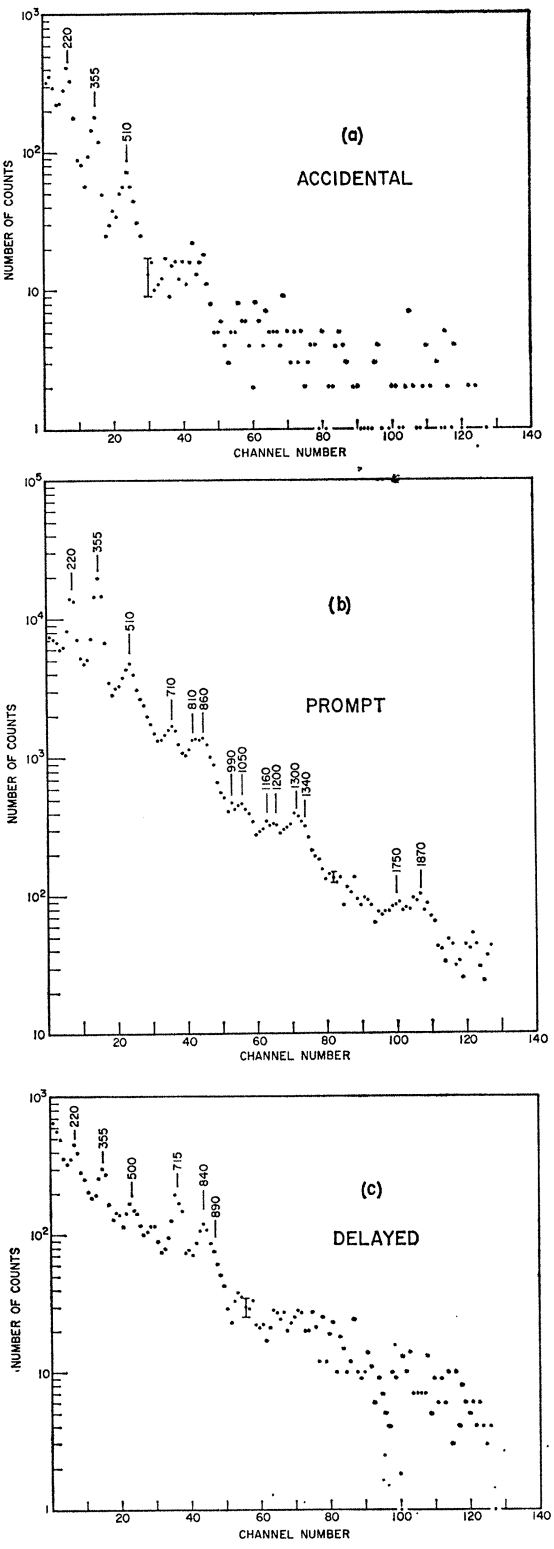

FIG. 18. Sintillation γ-ray spectra in (a) accidental, (b) prompt, and (c) delayed coincidence with 512-keV γ rays in the decay of Se^{83}.

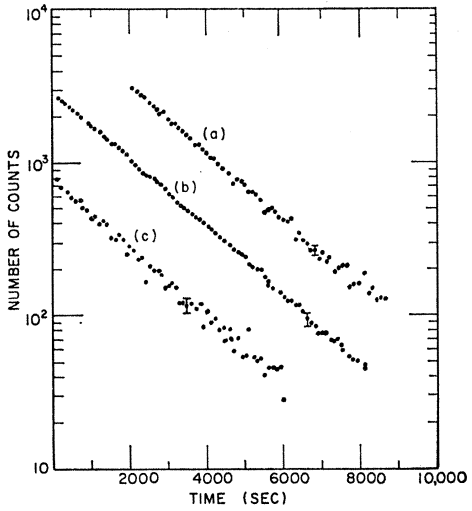

FIG. 19. Decay curves of the long-lived isomer of Se^{83}: (a) cadmium-covered sample, $E_\gamma=330$–370 keV; (b) chemically separated sample, $E_\gamma=300$–2400 keV; (c) coincident γ rays, $E_\gamma=400$–600 keV.

activation with a wetting agent containing sodium. The sample, activated and purified, was counted on a NaI(Tl) scintillation spectrometer with the single-channel analyzer set to accept γ rays in the energy region 300–2400 keV. The later part of the data, following the 15-h half-life of Na^{24}, was used to determine the Na^{24} background contribution which needed to be subtracted from the earlier part of the data. The resultant set of data points are indicated by (b) in Fig. 19. The origin of the time scale has been arbitrarily shifted for convenience in plotting the three sets of data. A least-squares analysis of these data resulted in $T_{1/2}=22.2\pm1.0$ min.

B. The Cadmium-Covered Sample

In another measurement, the sample was irradiated inside a cadmium cover which absorbed most of the incident thermal neutrons. Activation under these conditions was found to improve the ratio of 23-min to 70-sec Se^{83} activities, and therefore improve the ratio of 23-min Se^{83} activity to the 2.4-h Br^{83} activity which results from the decay of both isomers of Se^{83}. In addition, it suppressed the Na^{24} and Cl^{38} activities.

The single-channel analyzer of the NaI(Tl) scintillation spectrometer was set to accept γ rays in the energy region 330–370 keV (i.e., only the photopeak of the most prominent γ ray in the Se^{83} spectrum). The first counts used in the half-life determination were started 10 min after termination of the neutron exposure to avoid the effect of the 70-sec isomer. Counts taken prior to this time showed that the 70-sec activity would then be contributing less than 1% of the total counts. The source was counted for 24 h. Data taken near the end of this period indicated that a constant background of 178 counts per counting interval should be subtracted.

A least-squares analysis of the resultant data [indicated by (a) in Fig. 19] gave a value of $T_{1/2}=22.6\pm0.3$ min.

C. Coincident γ Rays

It was shown in Sec. VI that the 512- and 720-keV γ rays are in coincidence with each other and with the 837- and 886-keV γ rays. The time dependence of the intensity of coincident γ rays in this energy region should thus give a relatively clean indication of the lifetime of the long-lived isomer of Se^{83}.

The fast-slow coincidence system referred to in Sec. IV was modified so that a scaler-timer could be used to measure the half-life of a source emitting coincident radiations which were selected by each of the single-channel analyzers to be in the 400–600-keV energy region, while at the same time the multichannel analyzer recorded the γ-ray spectrum measured by detector No. 1 in coincidence with γ rays in the 400–600-keV region detected by No. 2. The 400–600-keV energy band was selected for each of the two detectors so as to include not only the photopeak of the 512-keV γ ray, but also substantial portions of the Compton distributions of the 720-, 837-, and 886-keV γ rays.

Since the energy of the 512-keV γ ray coincides within experimental error with that expected from positron annihilation, it was necessary to determine what portion of its intensity and the coincident intensity being measured might be due to annihilation of positrons and, if any, to determine the half-life of the activity producing the positrons.

The Se^{83} source was produced with thermal neutrons and the counting started 10 min after activation was stopped. The scintillation detectors were placed in a 180° geometry (separated by 2.8 cm and with the source midway between them) in order to reveal the possibile presence of positron activity. A series of coincident γ-ray spectra were recorded, each of the first three corresponding to an accumulation of data for approximately 20 min. Even during the second hour of decay the spectra could not be distinguished from the earlier scintillation coincidence data of Sec. VI obtained with the detectors at 90° with respect to each other. From the spectra recorded at the two different angles it was found that the ratio of the relative intensities of the 512- and 356-keV γ rays remained constant in time to with $\pm20\%$. After 3 h it became apparent that some positron activity was present, and continued measurements indicated a half-life of approximately 12 h. The contribution of the longer-lived positron activity to the 510-keV peak in the initial spectra was approximately 5%. It should be pointed out that this method (coincidence counting at 180°) greatly emphasizes positron annihilation counting as opposed to ordinary coincidence counting. In our case the detection of positron annihilation γ rays is emphasized by a factor of 6 in the 180° arrangement compared to the detection of coincident γ rays of the same energy. It is clear that any positron contribution is far too small to explain the presence of the 512-keV γ rays in the Se^{83} decay. The weak positron activity found was assigned on the basis of half-life to Cu^{64}($T_{1/2}=12.8$ h) or to pair production from the high-energy γ rays of Na^{24}($T_{1/2}=15.0$ h).

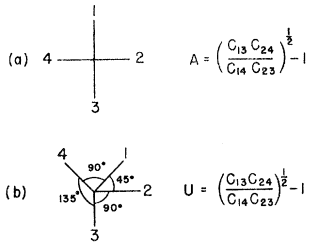

FIG. 20. Detector configurations used in directional correlation measurements.

With the contribution of a positron activity shown to be negligible, coincidence data for the 400–600-keV energy-selected bands for the two detectors was followed for 20 h. The later counts were used to determine the background (constant at 10 counts per interval) for the early and significant portion of the decay. A least-squares fit of the data, shown as (c) in Fig. 19, gave $T_{1/2}=22.6\pm0.5$ min.

D. Weighted Mean of the Three Lifetime Measurements

The standard errors computed in each of the three half-life determinations were used to provide weighting factors in the calculation of the weighted mean of the results and the standard error of the weighted mean. The result for the half-life of the long-lived isomer of Se^{83} is $T_{1/2}=22.6\pm0.2$ min.

X. γ-γ DIRECTIONAL CORRELATION MEASUREMENTS

The short half-life of Se^{83} makes directional correlation measurements difficult. In order to accumulate data rapidly and avoid corrections for decay of the source, directional correlations were performed with a four-detector apparatus, based on the one described by Gerholm, Lindqvist, and deWaard,[33] and by Lindqvist and Karlsson,[34] which permitted the coincidence count rate to be measured at two or more angles simultaneously. Although other configurations have been shown to be useful in special applications,[33,34] only the two shown in Fig. 20 were used in the present work. This choice results from the assumption that at least one of the two γ rays in each cascade does not contain octupole ($L=3$) and higher multipole radiation. (Otherwise, alternate modes of decay to other intervening levels would surely occur with higher probability, or else the lifetime of the intermediate level would be too long for a meaningful measurement.) With this assumption, the correlation function $W(\theta)$ contains terms in

[33] T. R. Gerholm, T. Lindqvist, and H. de Waard, Nucl. Instr. 1, 107 (1957).
[34] T. Lindqvist and E. Karlsson, Arkiv Fysik 12, 519 (1957).

$P_\nu(\cos\theta)$ no higher than those corresponding to $\nu=4$ and one needs to measure $W'(\theta)$ only at a sufficient number of angles to determine the constants A_2' and A_4' in the equation

$$W'(\theta)=1+A_2'P_2(\cos\theta)+A_4'P_4(\cos\theta), \quad (1)$$

where the primes indicate that geometrical corrections for detector size have not yet been included. The detectors, numbered 1–4, are equidistant from the radioactive source. In the configuration of Fig. 20(a), the coincidence count rates at 90° and 180° can be measured; and, in a separate measurement, the configuration in Fig. 20(b) allows the coincidence count rates at 90° and 135° to be measured. From these two separate measurements one obtains the data necessary for calculating the usual expressions for anisotropy:

$$A\equiv\frac{W'(180)}{W'(90)}-1, \quad (2)$$

$$U\equiv\frac{W'(135)}{W'(90)}-1, \quad (3)$$

in terms of which A_2' and A_4' can be expressed,[35]

$$A_2'=\frac{10(5A+4U)}{7(A+8U+15)}, \quad (4)$$

$$A_4'=\frac{48(A-2U)}{7(A+8U+15)}. \quad (5)$$

Lindqvist and Karlsson[34] have shown that small differences in efficiency and solid angle of the four detectors may be canceled out exactly in the analysis of the data. They show that this is true for the configuration displayed in Fig. 20(a) when

$$A\equiv\frac{W'(180)}{W'(90)}-1=\left[\frac{C_{13}C_{24}}{C_{14}C_{23}}\right]^{1/2}-1, \quad (6)$$

where C_{ij} represents the coincidence counts recorded between detectors i and j during a given experiment, and for the configuration in Fig. 20(b) when

$$U\equiv\frac{W'(135)}{W'(90)}-1=\left[\frac{C_{13}C_{24}}{C_{14}C_{23}}\right]^{1/2}-1. \quad (7)$$

Relations (6) and (7) permit the evaluation of the anisotropies A and U in terms of the coincidence count rates, while (4) and (5) permit the calculation of A_2' and A_4'. Finally, the coefficients A_2' and A_4' may be corrected for the finite detector size by the method of Rose[36,37] to obtain coefficients A_2 and A_4 which may be compared with theoretically predicted values.

The four detectors and their associated electronics were NaI(Tl) scintillation counters of the type described in Sec. VI. Six coincidence circuits were used to measure coincidences between the 6 possible combinations of pairs of detectors (although the data from only 4 were used in the data analysis). For each coincidence circuit there was a corresponding real-or-accidental coincidence selector.[29] To provide energy selection of coincident events, the detection of a coincidence between a certain pair of detectors opened an appropriate pair of linear gates so that the energy-dependent signals could be analyzed by two single-channel pulse-height analyzers set for the photopeak regions of the two γ rays of interest. The "crossed-delay" method of Gerholm *et al.*[33] was used to double the rate of data accumulation. A slow coincidence circuit gave an output signal when the selected energy condition had been met in some pair of detectors, and its output signal gated all real-or-accidental coincidence selectors so that an event could be appropriately counted as real or accidental. This provided the required continuous monitoring of the accidental contribution to the coincidence count rate.

Since the decay scheme of Se^{83} is such that there are interfering cascades for almost every cascade of interest, a technique was developed[38] for performing directional correlation measurements on a pair of γ rays γ_1 and γ_2 (with energy E_1 and E_2) when at least one (say γ_1) is part of a cascade containing an additional γ ray γ_3 (with energy E_3) such that E_3 is higher than E_2.

The directional correlation measurements were made on solid samples. Attenuation of the correlation is not expected to be a problem, however, since the delayed-coincidence measurements showed that the lifetimes of the intermediate levels was less than 10^{-9} sec and the magnetic dipole and electric quadrupole moments are not expected to be large.

To minimize the effects of interfering activities, six different samples of Se^{82} were irradiated and counted cyclically for the Br^{83} γ-ray directional correlations. Each sample was irradiated by neutrons for an appropriate time (usually 7 min), the short half-life activities were allowed to decay for 8 min, and then the sample was counted in the directional correlation apparatus for 45 min.

The source-to-detector distance was 4 cm and the source was approximately 1 mm in diameter. The centering of the source was determined from the count rate in each of the detectors. Slight adjustments in the source-to-detector distance were made to provide agreement of the count rates in the 4 detectors to within 1%. The

[35] F. Gimmi, E. Heer, and P. Scherrer, Helv. Phys. Acta **29**, 147 (1956).

[36] M. E. Rose, Phys. Rev. **91**, 610 (1953).

[37] H. I. West, Jr., University of California Radiation Laboratory (Livermore) Report No. UCRL-5451, 1959 (unpublished).

[38] K. W. Marlow (to be published).

calculations of Young[39] showed that source-dimension corrections to the correlation coefficients (A_2 and A_4) were negligible for the geometry used. Some Pb shielding was provided between adjacent detectors to reduce coincidence events due to scattering of γ rays from one detector to another.

A. The 512–356-keV Cascade

Using the techniques described, seven different measurements of the anisotropy A for the 512–356-keV cascade resulted in a mean value of $A_{\text{exp}}=-0.05\pm0.06$ (standard error of the mean). Similarly, 10 measurements of the anisotropy U resulted in $U_{\text{exp}}=-0.02\pm0.04$. From these values the coefficients A_2' and A_4' were determined and after applying the solid-angle correction we obtained $A_2=-0.04\pm0.04$ and $A_4=-0.01\pm0.06$.

A discussion of this and the following directional correlation result will be made in the context of other measurements in Sec. XI.

B. The "2300"–356-keV Cascade

Since the NaI(Tl) detectors cannot resolve the γ rays near 2300 keV, the peak at 2300 keV was treated as though it corresponded to one γ-ray transition in the "2300"–356-keV cascade, and no corrections were made for interfering cascades. Seven measurements of the anisotropy A resulted in a mean value of $A_{\text{exp}}=+0.005\pm0.003$. Similarly, 5 measurements of the anisotropy U resulted in $U_{\text{exp}}=-0.006\pm0.006$. The correlation coefficients (after apply the geometrical correction) were found to be $A_2=0.000\pm0.003$ and $A_4=+0.010\pm0.008$.

XI. DISCUSSION OF THE EXPERIMENTAL DATA

In this section all of the experimental results will be brought together to construct a consistent decay scheme for Se^{83}. The more accurate γ-ray results will be discussed first in order to have them available when interpretating the β-ray spectra. The total β-decay transition energy will then be deduced for each of the isomers in order to determine the energy separation of the isomeric levels. Possible limitations of the spin and parity of some levels will also be discussed.

A. Levels in Br^{83} Identified by the Observation of γ-Ray Transitions

1. Levels Populated by the Decay of the Long-Lived Isomer of Se^{83}.

In Sec. VI the excitation energy of a number of levels in Br^{83} was deduced from γ-γ coincidence-spectrum measurements reported in that section and from γ-ray singles spectrum measurements reported in Sec. IV. The delayed level (Sec. VIII) permitted an independent determination of the temporal order of several γ rays, results in full agreement with the conclusions drawn in Sec. VI. γ rays with energy 226, 356, 512, 720, 837, 868, 2291, and 2338 keV were shown to be transitions between various pairs of the levels at 0, 356, 868, 1094, 1814, 2650, and 2697 keV. The transitions and levels are shown on the proposed decay scheme (Fig. 21). The nine transitions account for 70% of the γ-ray intensity ascribed to the long-lived isomer. Relative intensity values from Table I are shown in parentheses after the energy notations (in keV) on Fig. 21. A prominent feature of the decay is the presence of the 5-step cascades (originating at the 2650- and 2697-keV levels), which are in common after the first step.

A level at 2777 keV has been proposed on the basis of a weak 2421-keV γ ray detected in the singles γ-ray spectra (Fig. 4) and in the spectrum in coincidence with the 356-keV γ ray (Fig. 9), but not detected in coincidence with the 512-keV γ ray (Fig. 10).

A more detailed study of the singles and coincidence γ-ray data, summarized in Tables I and III, has suggested levels in Br^{83} at 801, 1355, 1421, 1438, 2060, and 2738 keV. These levels, and the γ-ray transitions connecting them, are also shown on Fig. 21. In obtaining these levels and placing the γ rays associated with them, it was required that for each level: (1) at least two different γ-ray transitions into or out of the level gave an energy check on the level placement, (2) the singles intensity (Table I) of transitions into and out of the level balanced to within the quoted errors unless β-ray feeding of the level was expected, and (3) the placement of each γ ray connecting a pair of levels had to be supported by at least one coincidence measurement. Additional support for the placement of many γ rays was obtained from a balance of coincidence intensities, the sum-coincidence spectrum, and the scintillation coincidence spectra.

With the decay scheme shown in Fig. 21 we have been able to account for all of the γ rays listed in Table I except those at 487, 666, 1879, and 2088 keV. Each of these γ rays has a relative intensity less than 4 (normalized to 100 for the 356-keV γ ray). Hence the decay scheme of Fig. 21 accounts for 98% of the total γ-ray intensity of Table I. The 487-keV γ ray has the appropriate energy to be a transition between the levels at 1355 and 868 keV, and the coincidence data of Table III appear to confirm that the 487-keV γ ray is in coincidence with those at 356, 512, and 1344 keV. This placement of the 487-keV γ ray cannot be correct, however. If it were placed there, it would follow, as a consequence of the fact that the singles intensities of the 487-, 554-, and 1355-keV γ rays are approximately equal, that the column of Table III corresponding to coincidence with 1344-keV γ rays should indicate equal intensity for each of these three γ rays. Although the

[39] F. C. Young, U. S. Naval Research Laboratory Report No. 5475, 1960 (unpublished).

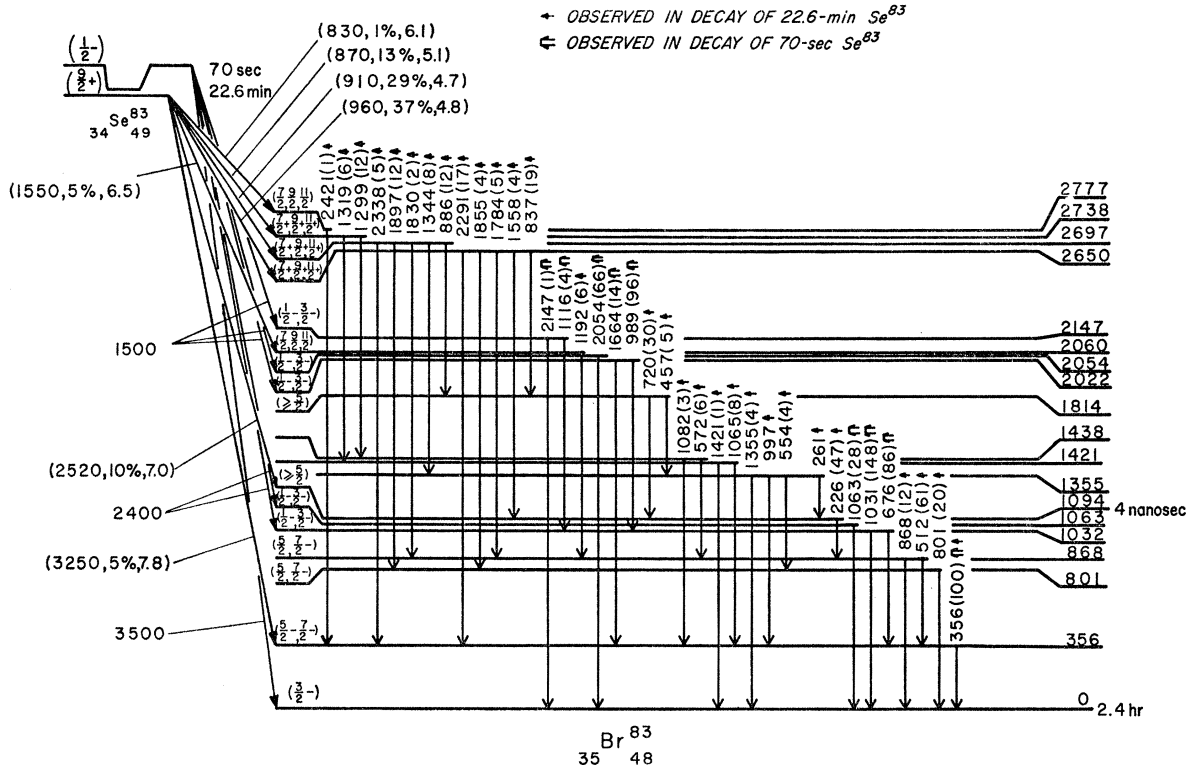

FIG. 21. Proposed decay scheme for Se^{83}.

values for the other two are approximately equal, the intensity of the 487-keV γ ray is much smaller. No satisfactory place in the decay scheme has been found for this γ ray.

The energy and coincident intensities listed in Table III for peaks at 874, 1270, and 1397 keV can be explained by considering these "γ rays" as the double-escape peaks of 1897-, 2291-, and 2421-keV γ rays. In addition, a double-escape peak of the 2338-keV γ ray occurs at nearly the same energy as that of the full-absorption peak of the 1319-keV γ ray. The intensities listed in Table I have been corrected for double-escape contributions, but those in Table III have not.

Several γ rays (each estimated to have $<2\%$ of the 356-keV γ-ray intensity) have been observed in the coincidence measurements but have not been placed in the decay scheme. They have the following energies: 296, 387, 416, 601, 610, 636, 1129, 1183, 1205, 1308, 1969, and 2046 keV.

2. *Levels Populated by the Decay of the Short-Lived Isomer of Se^{83}*

From the singles γ-ray spectra recorded with the germanium detector, the relative intensity was deduced (see Table II) for each of the γ rays observed following the decay of the short-lived isomeric state of Se^{83}. Although ordinary coincidence measurements have not been made, coincidence summing of γ rays in the well-type scintillation detector has provided spectra which show that the short-lived decay does not strongly populate levels in the 1100- to 1900-keV region nor in the region above 2100 keV, but does strongly populate levels near 1000 and 2000 keV. The 356-keV γ ray is the only one which we have observed in the decay of both isomers. On the basis of just these data, levels in Br^{83} are proposed at 0, 356, 1032, 2022, 2054, and 2147 keV. The placement of the 989- and 1063-keV γ rays requires an additional level, probably at 1063 or 989 keV. In the decay scheme shown in Fig. 21 the former choice is made and the 989-keV γ ray is represented as a transition between levels at 2022 and 1032 keV. An alternative assignment would be for the 1063- and 989-keV γ rays to form a cascade involving levels at 0, 989, and 2054 keV. With either assignment, intensity balance requires β-ray feeding of the level near 1000 keV. The β-ray spectrum measurements reported in Fig. 6 (and discussed more fully below) do not preclude this latter assignment, but the energy of the "2400"-keV transition (actually two or more transitions since the 1032-keV level is also populated by β decay) would indicate that feeding the level at 1063 keV is more probable than the lower-lying level at 989 keV.

B. β-Decay from the Se^{83} Isomeric Levels

An analysis of the β-decay data shown in Secs. V and VII can be used in an attempt to determine the

relative excitation energy of the isomeric levels in Se^{83} as well as to provide some limitation on the spins and parities of some of the levels of Br^{83}.

1. The Long-Lived Isomer

Utilizing the results of the analysis in Sec. A1 above, the net γ-ray intensity unbalance at a given level has been used to provide a measure of the intensity of β-ray transitions feeding that level. The levels at 2650 and 2697 keV are most strongly fed, and the β-ray spectrum measurements reported in Secs. V and VII indicate that the most intense β-ray transition has an end point of 930 ± 40 keV. Since the γ-ray intensity unbalance requires that this apparently simple observed β-ray spectrum be in fact a complex spectrum, the 930-keV value has been assumed to be the mean value of the end-point energies of 4 transitions (to the levels at 2650, 2697, 2738, and 2777 keV) whose relative intensities and energy separation are known from the intensity and energy measurements on the γ rays involved. On these bases the four β-ray transition energies were calculated to be 960, 910, 870, and 830 keV. Although such an analysis of the complex β-ray spectrum is lacking in rigor, the results are consistent with the decay scheme based on γ-ray measurements, the observed β-ray spectrum, and the small energy separation of the four groups, especially of the two groups with the greatest (and nearly equal) intensity. These two groups differ in energy by only 47 keV while the standard error of the mean value (930 keV) had been found to be 40 keV.

The calculated β-ray transition energy of 960 keV plus the excitation energy (2650 keV) of the level which it feeds, gives 3610 ± 40 keV for the total β-ray transition energy for the long-lived isomer. Since no β-ray transition of this energy (or within 300 keV of it) was observed for this isomer, it follows that all β-ray transitions feed excited levels in Br^{83}. Since each β-ray transition is followed by at least one γ ray, we may use the γ-ray intensity measurements to determine the percentage of the total β decay (branching) occurring for each of the different β-ray transitions. The β-ray intensity unbalance at various levels indicates that 7 β-ray transitions feed levels in Br^{83} at 356, 1094, 2060, 2650, 2697, 2738, and 2777 keV. (A weak transition to the 868-keV level cannot be excluded.) Using 3610 keV for the total disintegration energy, the β-ray transitions would have the following energies (and relative intensity): 3250 (5%), 2520 (10%), 1550 (5%), 960 (37%), 910 (29%), 870 (13%), and 830 (1%). (If a 2740-keV transition to the 868-keV level exists, its intensity is $<5\%$.) We have already discussed the last 4 transitions, which together account for 80% of the total β-ray intensity. The coincidence β-ray spectrum analyses reported in Sec. VII have confirmed the presence of the 1550- and 3250-keV transitions. And although the 2520-keV transition, if present, was obscured in the β-ray spectrum analyses, a scintillation γ-ray spectrum recorded with the source inside the well has independently confirmed the γ-ray unbalance and thus the β-ray feeding of the 1094-keV level by showing a sum peak which corresponds to that energy. The transition energy (in keV) and percentage branching for each of the 7 β-ray groups has been indicated in Fig. 21. The parentheses around these numbers in Fig. 21 indicates that the values given were obtained indirectly, i.e., from γ-ray energy and intensity measurements. The logft values for these β-ray transitions were calculated by the method of Moskowski,[40] and are indicated on the decay scheme as well as in Table V. From the study of Gleit *et al.*[41] of the frequency distributions of logft values of β-ray transitions for which the spin and parity changes are known and the logft values calculated above, the most probable spin and parity selection rules[42] for each transition have been deduced and are shown in Table V. These spin and parity changes should not be considered determined but rather useful checkpoints.

TABLE V. Energy, logft, and selection rules for the β-decay of the long-lived isomer of Se^{83}.

Energy (keV)	log ft	Spin change	Parity change
830	6.1	$0, \pm1$	Yes or No
870	5.1	$0, \pm1$	No
910	4.7	$0, \pm1$	No
960	4.8	$0, \pm1$	No
1550	6.5	$0, \pm1$	Yes or No
2520	7.0	$0, \pm1, \pm2$	Yes
3250	7.8	$0, \pm1, \pm2$	Yes

2. The Short-Lived Isomer

From the β-ray spectrum measurements reported in Sec. V, it was inferred that there are probably three β-ray transitions with energies 1500, 2400, and 3500 keV. The decay scheme based on the analysis of the γ-ray spectra, in particular the intensity unbalance of the γ rays into and out of the various levels, as discussed in Sec. XI A2, requires that there be more than three β-ray transitions. Since the isomeric levels in Se^{83} are expected to be closely spaced (no isomeric transition has been observed), a β-ray transition to the ground level of Br^{83} would be expected to have an energy close to the 3610 ± 40-keV total transition energy computed above for the long-lived isomer. The observed 3500 ± 100-keV β-ray transition is therefore proposed as the ground-level transition. Its energy is correct within the large errors; and the alternative would be to propose a low-lying excited level in Br^{83}, a level for which there

[40] S. A. Moskowski, Phys. Rev. **82**, 35 (1951).
[41] C. E. Gleit, C. W. Tang, and C. D. Coryell, *Nuclear Data Sheets*, compiled by K. Way *et al.* (Printing and Publishing Office, National Academy of Sciences—National Research Council, Washington, D. C.), NRC 5-5-109.
[42] C. S. Wu, *Nuclear Spectroscopy*, edited by F. Ajzenberg-Selove (Academic Press Inc., New York, 1960), Part A, p. 148.

has been no indication. The γ-ray energy and intensity results and the value of 3500 ± 100 keV for the total transition energy suggest that the "2400"-keV transition is composed of two transitions with slightly differing energies feeding levels at 1032 and 1063 keV; and the "1500"-keV transition to consist of three transitions which feed levels at 2022, 2054, and 2147 keV. Since the several modes of β-decay include a transition to the ground level, it was not possible to use γ-ray intensity unbalance at the various excited levels to determine the percentage of the total decay for the different β-ray transitions, and, as a consequence, the $\log ft$ values could not be calculated accurately. The $\log ft$ value for a given mode of decay is not a sensitive function of the percentage of decay occurring by this mode, however, a factor-of-two error in the percentage resulting in an additive error of 0.3 for the $\log ft$ value. If we make an estimate of the percentage branching to the ground level, the branching to the excited levels may be determined with fair accuracy from the γ-ray intensity unbalance at the excited levels. From Fig. 6 we observe that the 3500-keV transition occurs in a substantial percentage of the total β decay and we have estimated that this percentage lies in the range of 25 to 75%. We then find that the $\log ft$ values of all 6 transitions must lie correspondingly between 4.6 and 6.4 indicating that all 6 transitions are probably of the allowed type and therefore involve a spin change of 0 or ±1 and no change in parity.

C. The Spin and Parity of the Isomeric Levels

In order to establish the spin and parity of the isomeric levels of Se^{83}, we first establish the spin and parity of the ground level of Br^{83} and then use the β-ray selection rules in conjunction with shell-model predictions.

The shell model of the nucleus[43] predicts that the ground level of the odd-mass bromine isotopes should have $J\pi=\frac{3}{2}-$. $J=\frac{3}{2}$ has been confirmed for Br^{77} by measurements of Green *et al.*[44] and for Br^{79} and Br^{81} by measurements of King and Jaccarino.[45] By analogy it is assumed that the ground level of Br^{83} has $J\pi=\frac{3}{2}-$.

The odd-mass nuclei which contain 49 neutrons or protons fall into a category for which the ground and first excited levels are well-described by the shell model. The model predicts that for such nuclei the ground level has $J\pi=\frac{9}{2}+$ and a low-lying excited level has $J\pi=\frac{1}{2}-$. These predictions have been confirmed in 6 cases, and in 4 additional cases the known experimental data are best, but not uniquely, explained in this way. No exceptions have been found. An extrapolation of the variation with Z of the excitation energy of the $\frac{1}{2}-$ level above the $\frac{9}{2}+$ ground level for odd-mass 49-neutron nuclei[46] indicates that for Se^{83} ($Z=34$) the excitation energy would be approximately 100 keV.

Recently, Lin[47] excited the $\frac{9}{2}+$ level of Se^{83} by means of the $Se^{82}(d,p)Se^{83}$ reaction and measured the Q value of the reaction to be 3750 ± 50 keV. Combining this information with the Q value for the $Se^{82}(p,\gamma)Br^{83}$ reaction[48] gives a value for the total β-decay energy between the $\frac{9}{2}+$ level of Se^{83} and the ground level of Br^{83} of 3580 ± 50 keV. Lin also identified a $\frac{1}{2}-$ level in Se^{83} with an excitation energy 220 ± 40 keV above the $\frac{9}{2}+$ level.

For the purpose of comparison with the results of the present experiment we assume that Se^{83} has two closely spaced levels (within approximately 200 keV) with $J\pi=\frac{9}{2}+$ and $\frac{1}{2}-$, as predicted by the shell model. β-ray transitions from these two levels to the ground level of Br^{83} would be classified as third-forbidden and allowed, respectively. We have observed an allowed transition to the ground level of Br^{83} for the 70-sec decay of Se^{83}, but have failed to observe any β-ray transitions to the ground level of Br^{83} for the 23-min decay of Se^{83}. Therefore, we propose that the level which decays with $T_{1/2}=70$ sec has $J\pi=\frac{1}{2}-$ and the level which decays with $T_{1/2}=23$ min has $J\pi=\frac{9}{2}+$. In Sec. XI B, we have shown that the $\frac{9}{2}+$ level decays by at least 3 allowed transitions to levels in Br^{83} at approximately 2700 keV. According to the rules for allowed β decay,[42] these levels would have $J\pi=\frac{7}{2}+$, $\frac{9}{2}+$, or $\frac{11}{2}+$. Further, the selection rules for γ-ray emission[49] show that γ-ray transitions from any of these levels directly to the $\frac{3}{2}-$ ground level would be strongly hindered, resulting in preferential decay by means of cascading transitions through one or more intermediate levels with $J\pi=\frac{3}{2}+$, $\frac{5}{2}+$, $\frac{5}{2}-$, or $\frac{7}{2}-$. The results of the present experiment which show that the levels near 2700 keV do not decay by transitions directly to the ground level, but decay only by cascades of two or more transitions, provide further confirmation for the proposal that the level in Se^{83} which decays with $T_{1/2}=23$ min has $J\pi=\frac{9}{2}+$.

Although it would be of interest to determine the energy difference for the $J\pi=\frac{1}{2}-$ and $\frac{9}{2}+$ levels in Se^{83}, we have been unable to do so. The total decay energy to the ground level of Br^{83} for the short-lived ($J\pi=\frac{1}{2}-$) isomer has been found to be 3500 ± 100 keV while this energy difference for the long-lived isomer ($J\pi=\frac{9}{2}+$) has been found to be 3610 ± 40 keV. These values, along with their respective errors, have a region of overlap

[43] M. Goeppert-Mayer and J. H. D. Jensen, *Nuclear Shell Structure* (John Wiley & Sons, Inc., New York, 1955), pp. 74–85.
[44] T. M. Green, H. Garvin, E. Lipworth, and K. Smith, Bull. Am. Phys. Soc. 4, 250 (1959).
[45] J. G. King and V. Jaccarino, Phys. Rev. 94, 1610 (1954).
[46] *Nuclear Data Sheets*, edited by K. Way *et al.* (Printing and Publishing Office, National Academy of Sciences—National Research Council, Washington, D. C.).
[47] E. K. Lin, Phys. Rev. 139, 340 (1965).
[48] J. H. E. Mattauch, W. Thiele, and A. H. Wapstra, Nucl. Phys. 67, 32 (1965).
[49] S. A. Moskowski, *Beta- and Gamma-Ray Spectroscopy*, edited by K. Siegbahn (North-Holland Publishing Company, Amsterdam, 1955), pp. 373–395.

so that we cannot determine which level lies at the lower energy; they indicate, however, that the $\frac{1}{2}-$ level probably does not lie more than 30-keV above the $\frac{9}{2}+$ level. In order to be consistent with the theoretical prediction and the systematic study of neighboring nuclei, we have represented the $\frac{1}{2}-$ level above the $\frac{9}{2}+$ level in the proposed decay scheme of Fig. 21. Our results indicate that the $\frac{1}{2}-$ isomeric level cannot lie as far above the $\frac{9}{2}+$ ground level as the $\frac{1}{2}-$ level (at 220 keV) found by Lin.[47] Therefore, we suggest that the isomeric level was sufficiently weakly excited and sufficiently close in energy to the $\frac{9}{2}+$ level that Lin was unable to observe it.

D. The Spin and Parity of Levels in Br^{83}

Taking the spins and parities of the ground level of Br^{83} and the isomeric levels of Se^{83} as established, it is of interest to try to assign (or at least place limits on) the possible values of the spin and parity of some of the excited levels in Br^{83}. In order to do this, we have used all features of the observed β and γ decay, the directional correlation results reported in Sec. X, the β-decay selection rules, and the observed relative γ-ray transition rates.

The results of detailed arguments based on these data are summarized in Table VI and indicated on Fig. 21. Indications of the principal data used are given in the third column, except for the information about the spin and parity of the relevant state of Se^{83} and the assumption that the spin of Br^{83} in the ground state is $\frac{3}{2}-$. In some cases assignments are included within parentheses.

TABLE VI. Assignment of spins and parities to levels of Br^{83}.

Level in Br^{83}	Spin and parity	Principle bases of assignment
2777	$\frac{7}{2}$, $\frac{9}{2}$, $\frac{11}{2}$	β
2738	$\frac{7}{2}+$, $\frac{9}{2}+$, $\frac{11}{2}+$ all different	β; γ, γ branching
2697	$\frac{7}{2}+$, $\frac{9}{2}+$, $\frac{11}{2}+$	β; γ, dir. corr., γ branching
2650	$\frac{7}{2}+$, $\frac{9}{2}+$, $\frac{11}{2}+$	β; γ, dir. corr., γ branching
2147	$\frac{1}{2}-$, $\frac{3}{2}-$	β
2060	$\frac{7}{2}\pm$, $\frac{9}{2}\pm$, $\frac{11}{2}\pm$	β
2054	$\frac{1}{2}-$, $\frac{3}{2}-$	β
2022	$\frac{1}{2}-$, $\frac{3}{2}-$	β
1814	$\frac{5}{2}\pm$, $\frac{7}{2}-$, $\frac{9}{2}-$, $\frac{11}{2}-$, $(\frac{13}{2}\pm)$	no β; γ, γ branching
1438	$\frac{3}{2}+$, $\frac{5}{2}\pm$, $\frac{7}{2}-$, $\frac{9}{2}-$, $\frac{11}{2}$	no β; γ
1421	$\frac{3}{2}+$, $\frac{5}{2}\pm$, $\frac{7}{2}-$, $\frac{9}{2}-$	no β; γ
1355	$\frac{3}{2}+$, $\frac{5}{2}\pm$, $\frac{7}{2}-$	no β; γ
1094	$\frac{7}{2}-$, $\frac{9}{2}-$, $\frac{11}{2}-$, $(\frac{5}{2}-$, $\frac{7}{2}+$, $\frac{9}{2}+$, $\frac{11}{2}+$, $\frac{13}{2}-)$	β; γ
1063	$\frac{1}{2}-$, $\frac{3}{2}-$	β
1032	$\frac{1}{2}-$, $\frac{3}{2}-$	β
868	$\frac{5}{2}\pm$, $\frac{7}{2}-$, $(\frac{3}{2}+)$	no β; γ, γ branching, dir. corr.
801	$\frac{5}{2}\pm$, $\frac{7}{2}-$	no β; γ, γ branching
356	$\frac{5}{2}-$, $\frac{7}{2}-$	β; γ
0	$\frac{3}{2}-$	

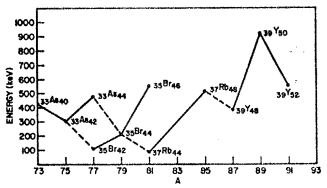

FIG. 22. Energy difference between the $\frac{9}{2}+$ and ground levels, plotted versus mass number A for odd-even nuclei with $33 \leqslant Z \leqslant 39$.

This notation indicates an assignment which is not excluded by the data, but which is unlikely on the basis of the data.

A systematic study of odd-Z even-N nuclei with $33 \leq Z \leq 39$ has shown that many of these nuclei have levels with $J\pi = \frac{9}{2}+$ lying a few hundred keV above the ground level.[46] A plot of the excitation energy of these $\frac{9}{2}+$ levels versus mass number (A) is shown in Fig. 22. Solid lines connect points corresponding to isotopes and broken lines connect isotones. Extrapolation of these experimental data suggests that a $\frac{9}{2}+$ level should appear in Br^{83} with an excitation of 800 to 1100 keV. Although the delayed level at 1094 keV might be identified as the $\frac{9}{2}+$ level, such an assignment is of no advantage in explaining the unique features of the decay scheme and, indeed, further complicates the attempt to explain the experimentally observed β- and γ-ray transitions. If a low-lying $\frac{9}{2}+$ level exists in Br^{83}, it would undoubtedly be strongly populated by β decay from the $\frac{9}{2}+$ level of Se^{83}, but no such level has been identified. (It would be of interest to check the assignment of the $\frac{9}{2}+$ levels in the neighboring nuclei. Some of these assignments have been based on analogous levels in other nuclei for which the assignment was based primarily on the lifetime of the level.)

XII. COMPARISON OF EXPERIMENTAL RESULTS WITH THE CORE-EXCITATION MODEL

There are various versions of the core-excitation model of the nucleus with which the experimental data on $_{35}Br_{48}^{83}$ might be compared. According to these models some excited levels of odd-A nuclei result from the coupling of the odd particle to the ground state or an excited state of the even-even core. One can, in principle, treat such an interaction rather generally,[2] but the detailed calculations required for comparison of theory and experiment have required approximations and/or limitations on the problem and the choice of these has resulted in the various versions of the model.

For $_{35}Br_{48}^{83}$ the core nucleus would be $_{34}Se_{48}^{82}$. Though the neutron number is near that for a closed shell the proton number is not and one might expect such a core to have a quadrupole deformation.[50] Indeed, the measured quadrupole moments of even-N nuclei

[50] O. Nathan and S. G. Nilsson, *Alpha-, Beta-, and Gamma-Ray Spectroscopy*, edited by K. Siegbahn (North-Holland Publishing Company, Amsterdam, 1965), p. 616.

with $Z=33$, 35, and 37 lead to predictions of significantly large deformation for these nuclei.[51]

The systematics of nuclei near Br^{83} and the proposed decay scheme indicate that the odd proton in this case should be a $p_{3/2}$ particle. The $p_{1/2}$ and $f_{5/2}$ single-particle orbitals are the ones which might be expected to admix. These are the same orbitals included in the description of $_{29}Cu_{34}^{63}$, the nucleus which has served as the test case for most of the previous core-excitation model calculations. But, unfortunately, the parameters for the $_{28}Ni_{34}^{62}$ core are built into these previous calculations in a manner which makes it difficult to compare the theoretical results with another test case without carrying out the calculations from almost the beginning. In addition, the core of Cu^{63} occurs at the closure of a minor shell for protons. We have attempted to do what seemed possible in the way of comparison of Br^{83} with the models (in particular, those of Thankappan and True,[8] Beres,[9] and Bayman and Silverberg[5]), short of repeating the work of several theoretical papers. Only with the theory of Bayman and Silverberg were we able to show meaningful detailed relations between the experimental results and theory. We attempt to show some of these relations below.

Bayman and Silverberg[5] solved exactly the particular problem of the coupling of a $J=\frac{3}{2}$ particle to an even-even core which can undergo surface vibrations. The coupling is via a quadrupole-quadrupole interaction and all orders of core excitation are included.

A. Excitation Energy of Negative-Parity Levels

In order to compare the predictions of Bayman and Silverberg with the results of the present experiment, we converted their energy scale from units of $\hbar\omega$ to units of keV, using the measured[52] value of the excitation energy of the one-phonon (2+) state in the even-even core (Se^{82}): 654 keV. We then found the value of coupling strength which would lead to a prediction of 356 keV for the first excited level (using Fig. 1 of Bayman and Silverberg[5]). The value is found to be $y\approx 0.9$. The theory predicts that with this intermediate coupling strength 3 approximately degenerate levels (with $J=\frac{1}{2}$, $\frac{5}{2}$, and $\frac{7}{2}$) should be found instead of the one isolated level actually observed at 356 keV (with $J=\frac{5}{2}$ or $\frac{7}{2}$). In view of further comparisons, however, it will be suggested that the 356-keV level (as the predicted $J=\frac{5}{2}$ level) is the first excited level of a ground-state quasirotational band, and the $J=\frac{1}{2}$ and $\frac{7}{2}$ levels either do not exist or have not been populated in this study. Indeed, Bayman and Silverberg suggest that the $J=\frac{5}{2}$ level should be the most strongly populated of the three.

In considering further the consequences of the coupling strength $y\approx 0.9$, we find that a number of approximately degenerate levels are predicted at 840 keV. Of these, one level is the $J=\frac{7}{2}$ member of the ground-state band, and the remaining levels have $J=\frac{9}{2}$, $\frac{3}{2}$, $\frac{11}{2}$, and $\frac{5}{2}$. Two levels have been found experimentally in this energy region (at 801 and 868 keV), each level having been identified with $J=\frac{5}{2}$ or $\frac{7}{2}$. If we identify one of the experimentally observed levels with the $J=\frac{7}{2}$ member of the ground-state band, then it is proposed that the other level be identified as the theoretically predicted $J=\frac{5}{2}$ level. Additional discussion of these levels is included below. The predicted $J=\frac{9}{2}$ and $\frac{3}{2}$ levels are each the second members of $K=\frac{7}{2}$ and $K=\frac{1}{2}$ bands for which we have already noted the absence of the lowest members; and furthermore, we have been unable to identify these higher members. The $J=\frac{5}{2}$ and $\frac{11}{2}$ levels correspond to the lowest members of new bands of levels with $K=\frac{5}{2}$ and $\frac{11}{2}$, respectively. The $J=\frac{11}{2}$ level has not been identified.

The next predicted level (at 930 keV) is the $J=\frac{3}{2}$ ($r=1$) level associated with the first vibrational level in the nucleus. [In their theory, Bayman and Silverberg define r as a "principal" quantum number indicating that a given state is the $(r+1)$-lowest state which otherwise possesses the same symplectic transformation properties.] This level could possibly be identified with either the 1032- or 1063-keV level, for each of which we have proposed $J=\frac{1}{2}$ or $\frac{3}{2}$.

By extrapolating the plots of Bayman and Silverberg, we find that the next predicted group of nearly degenerate levels occur at 1320 keV and have $J=\frac{9}{2}$, $\frac{11}{2}$, $\frac{5}{2}$, $\frac{13}{2}$, $\frac{7}{2}$, $\frac{15}{2}$, $\frac{9}{2}$, and $\frac{3}{2}$. The $J=\frac{11}{2}$, $\frac{5}{2}$, and $\frac{13}{2}$ levels correspond to higher members of bands whose lower members have not been observed. The first $J=\frac{9}{2}$ level and the $J=\frac{7}{2}$ level correspond to excited levels of the $K=\frac{3}{2}$ and $K=\frac{5}{2}$ bands which we have (at least tentatively) identified. At almost the same energy (1370 keV) the $r=1$ group of levels with $J=\frac{1}{2}$, $\frac{5}{2}$, and $\frac{7}{2}$ are predicted. There remain 5 experimentally determined levels (in the energy region 1000 to 1500 keV) which might be identified with some of these theoretically predicted levels.

In deformed nuclei, transitions between levels of different rotational bands are strongly hindered, but transitions between levels within a given rotational band are not hindered. In the experimental data summarized in the proposed decay scheme of Fig. 21, we find a sequence of levels which provides remarkable agreement with the theoretically predicted energies as well as a preference for what appear to be intraband transitions. These levels occur at 0, 356, 868, and 1438 keV. They have been identified with the $K=\frac{3}{2}$ ground-state band of levels having the spin sequence $\frac{3}{2}$, $\frac{5}{2}$, $\frac{7}{2}$, and $\frac{9}{2}$, with theoretically predicted excitation energies 0, 356, 840, and 1320 keV. Considering the energy agreement and the strong intraband transition to the 356-keV level, the 868-keV level has been identified with $J=\frac{7}{2}$ and the

[51] M. A. Preston, *Physics of the Nucleus*, (Addison-Wesley Publishing Company, Inc., Reading, Massachusetts, 1962), pp. 66–68.

[52] P. H. Stelson and F. K. McGowan, Nucl. Phys. **32**, 652 (1962).

1438-keV level with $J=\frac{9}{2}$. This leaves $J=\frac{5}{2}$ as the proposed assignment for the 801-keV level. Since the 1355-keV level decays preferentially to the 801-keV level rather than other excited levels, we propose that these are the $J=\frac{7}{2}$ and $\frac{5}{2}$ levels in the $K=\frac{5}{2}$ band which originates at 801 keV.

Similarly, we may identify the 1094-keV level as the beginning of a $K=\frac{9}{2}$ band. From the remaining theoretically predicted levels this is the only reasonable choice, since other selections would require the lifetime of the level and/or the mode of decay to be drastically different from what we have observed. Further, the 1094-keV level is populated almost entirely by a 720-keV transition from a level at 1814 keV; this behavior being of the type associated with a transition from the first excited level to the ground level of a rotational band.

One point must be considered, however. The identification of the 1094-keV level with $J=\frac{9}{2}$ leads to $J=\frac{11}{2}$ for the 1814-keV level. Extrapolation of the data of Bayman and Silverberg indicates that the next group of levels (which would include the $J=\frac{11}{2}$ level) lies at approximately 1850 keV. Since the 1094-keV level is almost half way between the theoretically predicted levels at 840 and 1320 keV, one might wish to consider the identification of the 1094- and 1814-keV levels as the $J=\frac{11}{2}$ and $\frac{13}{2}$ members of the $K=\frac{11}{2}$ band which would originate near 840 keV. We have discarded this possibility, however, for we find that at least one of the levels at 2650 and 2697 keV has $J\pi=\frac{7}{2}+$ or $\frac{9}{2}+$, and these levels decay much more strongly to the 1814-keV level than to the 1094-keV level. If we were to propose $J\pi=\frac{13}{2}-$ for the 1814-keV level and $J\pi=\frac{11}{2}-$ for the 1094-keV level, we would have the problem of explaining why the transitions to the 1814-keV level are more probable than the lower-multiple, higher-energy crossover transitions to the 1094-keV level. If, on the other hand, the 1814- and 1094-keV levels are the lowest two members of a $K=\frac{9}{2}$ band, we have the possibility that the stopover transition to the 1814-keV level could have the *same* multipolarity as the crossover transition to the 1094-keV level. Although it is a lesser problem, we have been unable to explain why the higher-energy crossover transition is less probable than the stopover transition.

Only one of all of the remaining theoretically predicted levels near 1850 keV has been identified, the level at 2060 keV. Although we suggest that it is the $J=\frac{9}{2}$ member of the $K=\frac{5}{2}$ band, it could perhaps be equally well identified as the $J=\frac{11}{2}$ member of the ground-state $K=\frac{3}{2}$ band.

Figure 23 shows a comparison of the levels of Br^{83} with the theoretically preedicted levels discussed here. The $K=\frac{3}{2}$, $\frac{5}{2}$, and $\frac{9}{2}$ bands are illustrated separately, while the remaining observed negative-parity levels are shown along with some other theoretically predicted levels of interest. Although we have attempted to demonstrate further comparisons of "other experimental levels" with the "other predicted levels," the results have been more ambiguous than for the cases we have described.

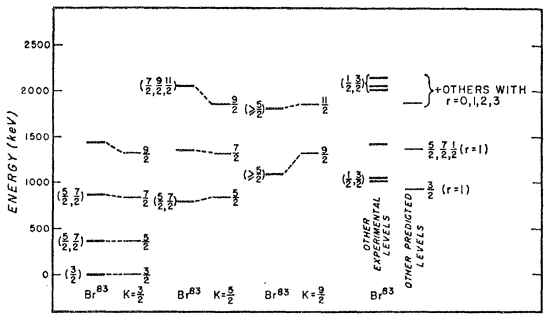

FIG. 23. A comparison of the observed levels in Br^{83} below 2200 keV and some of the levels predicted by the theory of Bayman and Silverberg (Ref. 5). The experimentally determined levels are identified by Br^{83} and the spins inferred by this work are given in parentheses on the left. The bands of levels predicted by Bayman and Silverberg (with $y=0.9$ and $\hbar\omega=654$ keV) are identified by the K quantum numbers, with spin designations to the right of each level. Additional bands of levels are predicted by the theory, but are not shown on the figure since no corresponding levels were observed in Br^{83}.

For the ground-state $K=\frac{3}{2}$ band and the additional $K=\frac{3}{2}$ band (with $r=1$), the only possible relation beteeen K and S is with $K=2S+\frac{3}{2}$.[53] For $S=1$ or 2 the relation $K=2S-\frac{3}{2}$ is also possible, and with $S=3$ a third possibility, $K=2S-\frac{9}{2}$, occurs. If the levels have been accurately identified above, we find that no bands at all have been observed for $S=1$; and for $S=2$ and 3, only those bands occur which correspond to the relation $K=2S-\frac{3}{2}$.

Although the comparison of the levels of Br^{83} with the theoretical predictions is most meaningful for the intermediate coupling, it is interesting to make some observations based on the assumption of strong coupling. According to Bayman and Silverberg, if it were not for extensive mixing of bands in the strong-coupling limit, the $K=\frac{3}{2}$ and $\frac{9}{2}$ bands should follow the $J(J+1)$ rule and the $K=\frac{5}{2}$ band should follow a $J(J+3)$ rule. Using the two lowest levels in each of these three bands, we have determined the moment of inertia parameter (as it is frequently expressed)

$$\begin{aligned} 3\hbar^2/\Im &= 427 \text{ keV}, \quad K=\tfrac{3}{2} \\ &= 371 \text{ keV}, \quad K=\tfrac{5}{2} \\ &= 390 \text{ keV}, \quad K=\tfrac{9}{2}. \end{aligned}$$

These values are approximately 4 times larger than those observed for the strongly deformed nuclei in the mass region $150<A<180$, and correspond to a smaller moment of inertia for Br^{83}. Extending the $J(J+1)$ rule

[53] Bayman and Silverberg (Ref. 5) relate K and S by

$$K=2S+\tfrac{3}{2},\ 2S-\tfrac{3}{2},\ \cdots \begin{matrix}\tfrac{1}{2} \\ \tfrac{3}{2} \\ \tfrac{5}{2}\end{matrix},$$

where $S=0$, 1, 2, $\cdots$. The unobserved $K=\frac{1}{2}$ and $\frac{7}{2}$ bands, for example, correspond to $S=1$.

for the ground-state band, and calculating the energy of other members of the band, one obtains 854 and 1495 keV for the $J=\frac{7}{2}$ and $\frac{9}{2}$ members, respectively. These values are in somewhat better agreement with those of the 868- and 1438-keV levels than the values which were calculated with $y=0.9$. Similarly, the $J=\frac{9}{2}$ member of the $K=\frac{5}{2}$ band would be predicted at 2040 keV, in much better agreeement with the value for the observed 2060-keV level than the 1850-keV value predicted with $y=0.9$. Although interesting, it is difficult to justify these strong-coupling considerations without a large increase in the value of the one-phonon excitation energy of the core.

B. Transition Rates

Although Harvey[6] has computed some transition rates from some of the low-lying levels to the ground level as a function of coupling strength in the Bayman and Silverberg model, transition rates to *excited* levels were not computed. In order to make a comparison betweeen theory and experiment, it will be assumed that the quasirotational bands discussed above are purely rotational and, hence, branching ratios for transitions between different rotational bands may be calculated by a formula given by Elliott[54]:

$$\frac{B(\lambda: J_i \rightarrow J_f')}{B(\lambda: J_i \rightarrow J_f)} = \frac{[J_i \lambda K_i (K_f - K_i) | J_f' K_f]^2}{[J_i \lambda K_i (K_f - K_i) | J_f K_f]^2}$$

for the ratio of the reduced transition probabilities $B(\lambda: J_i \rightarrow J_f)$ in terms of the squares of Clebsch-Gordon coefficients. For the assignment of $K=J=\frac{5}{2}$ for the 801-keV level and $K=J=\frac{3}{2}$ for the 1032-keV level, some calculated branching ratios are compared with experimental results and single-particle estimates in Table VII. In each case we have assumed that the ground and 356-keV levels are the corresponding levels of a $K=\frac{3}{2}$ band and that the transitions are of the $M1$ type. In each case the interband-transition calculation gives no better agreement with experiment than does the single-particle estimate.

Transitions from the proposed $K=\frac{9}{2}$ band to the $K=\frac{3}{2}$ ground-state band would involve $\Delta K=3$. A simple estimate of the branching from the 1094-keV level to the first and second excited levels in the ground state band is not available for $\Delta K=3$ transitions, but empirical data show that transitions are generally retarded by a factor of 10 to 100 for each degree of K forbiddeness. Although the single-particle estimate agrees with experiment for the branching of the 1094-keV level, that estimate predicts $T_{1/2}=3\times10^{-12}$ sec for the lifetime of the level. The measured lifetime, $T_{1/2}=4.1\times10^{-9}$ sec, is approximately 3 orders of magnitude larger, in good agreement with our suggestion of third-order K forbiddeness for transitions from the 1094-keV level.

TABLE VII. Branching ratio for various levels in Br^{83}.

Initial level energy (keV)	γ rays depopulating initial level γ_1 (keV)	γ_2 (keV)	(Intensity of γ_1)/(Intensity of γ_2) Experiment	Theory Shell model[a]	Theory Pure rotational[b]	Initial, intermediate, and final spin values
801	445	801	0 ±0.05	300		$\frac{7}{2}, \frac{5}{2}, \frac{3}{2}$
				0.16	0.07	$\frac{5}{2}, \frac{5}{2}, \frac{3}{2}$
868	512	868	5.0±0.7	300		$\frac{7}{2}, \frac{5}{2}, \frac{3}{2}$
				0.20		$\frac{5}{2}, \frac{5}{2}, \frac{3}{2}$
1032	676	1032	0.6±0.1	0.24	0.19	$\frac{3}{2}, \frac{5}{2}, \frac{3}{2}$
				1.4×10^{-4}		$\frac{1}{2}, \frac{5}{2}, \frac{3}{2}$
1063	707	1063	0 ±0.06	0.24		$\frac{3}{2}, \frac{5}{2}, \frac{3}{2}$
				1.4×10^{-4}		$\frac{1}{2}, \frac{5}{2}, \frac{3}{2}$
1094	738	226	0 ±0.06	0.02		$\frac{9}{2}, \frac{7}{2}, \frac{5}{2}$

[a] Single-particle shell-model estimates (Ref. 49).
[b] Interband transitions calculated for strong-coupling rotational model assuming $M1$ transitions only (Ref. 54).

[54] J. P. Elliott, University of Rochester Report No. NYO-2271, 1958 (unpublished).

XIII. CONCLUSIONS

Beta- and gamma-ray spectroscopic techniques have been used in a study of the 70-sec and 22.6-min activities of Se^{83}. The results of this experimental work have led to the construction of a proposed decay scheme with 18 excited levels in Br^{83}.

The excited levels of Br^{83} have been shown to agree in certain respects with collective motion of medium-mass nuclei. The 14 lowest excited levels in Br^{83} show a close correspondence with levels predicted by the model of Bayman and Silverberg[5] using an intermediate coupling ($y\approx0.9$). At least three rotational-type bands of levels have been tentatively identified. The delayed character of the level at 1094 keV has been interpreted as arising from K-forbidden transitions. Similar delayed levels in other odd-mass bromine isotopes should be reinvestigated to explore further the possibility of K-forbidden transitions in medium-mass nuclei.

ACKNOWLEDGMENTS

The authors would like to express their appreciation for assistance in various aspects of this work. Arlo D. Anderson developed the digital computer program for backscattering correction and Fermi analysis of the β-ray spectra. Dr. Conrad H. Cheek performed the chemical separations used to confirm the selenium activity. Some of the early measurements with a Ge(Li) detector were provided by James D. Ritter. David M. Shores performed many important tasks, including construction of electronic circuits and neutron irradiation of samples. Finally, we would like to thank Dr. J. O. Elliot and Dr. C. V. Strain for continued encouragement and support of the work.